2021-12

Investigation of metallic iron for water defluoridatio

Lufingo, Mesia

NM-AIST

INVESTIGATION OF METALLIC IRON FOR WATER DEFLUORIDATION

Mesia Lufingo

A Dissertation Submitted in Partial Fulfillment of the Requirements for the Degree of Master's in Environmental Science and Engineering of the Nelson Mandela African Institution of Science and Technology

Arusha, Tanzania

December, 2021

ABSTRACT

Fluorosis is a significant ailment that affects millions of humans and animals, especially in low-income countries. It has been the focus of past and present scientific endeavours to research and develop efficient and deployable technologies, especially in these low-income communities. In this work, metallic Iron (Fe^0) is a promising technology, and its filters have successfully addressed both safe drinking water and sanitation and are frugal. The recalled science of Fe^0 filters is demonstrated with the lingering design investigations. This study aimed at the critical assessment on defluoridation efficiencies under conventional metallic iron aqueous systems; where at first, Fe^0 materials were characterized with 1,10 Phenanthroline (Phen) in aqueous condition, and later batch studies were realized at the laboratory scale for two days under varied experimental conditions of: (a) 0.1 g and 1.0 g of iron mass, (b) Equimolar contamination, 23±2.0 mg/L, of co-solutes, i.e. NO_3, PO_4, SO4, HCO_3, Cl, (c) Initial pH values of 4.5, 7.0 and 9.5, and (d) Disturbed and non-disturbed treatments. Characterization results proved the potential of 1,10-Phenanthroline as a sole Fe^0 novel and facile characterization method. Defluoridation results revealed a maximum of 94% and 47% for quantitative (involving co-precipitation, adsorption and occasionally size-exclusion remediations) and non-quantitative (associated with adsorption as major remediation means) fluoride removal efficiencies, respectively. Thus, a conventional metallic iron aqueous system requires incorporating suggested nano-scale practices towards enhancing efficiency for affordable defluoridation achievements in future continuous system designs.

DECLARATION

I, Mesia Lufingo do hereby declare to the Senate of The Nelson Mandela African Institution of Science and Technology that, this dissertation is my original work and that it has neither been submitted nor being currently submitted for degree award in any other institution.

Mesia Lufingo

Name and Signature of Candidate Date

Prof. Karoli N. Njau

Name and Signature of Supervisor 1 Date

Prof. Chicgoua Noubactep

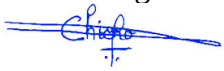

Name and Signature of Supervisor 2 Date

COPYRIGHT

CERTIFICATION

The undersigned certify that have read and hereby recommend for acceptance by the Senate of the Nelson Mandela African Institution of Science and Technology, a dissertation entitled *"Investigation of metallic Iron for Water Defluoridation"* in Partial Fulfilment of the Requirement for the Degree of Master's in Environmental Science and Engineering of the Nelson Mandela African Institution of Science and Technology.

Prof. Karoli N. Njau

Name and Signature of Supervisor 1 Date

Prof. Chicgoua Noubactep

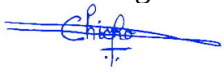

Name and Signature of Supervisor 2 Date

ACKNOWLEDGEMENTS

I dedicate my sincere acknowledgements to my almighty god, my family, and my academic and non-academic friends/colleagues for their direct and indirect assistance during my master's studies at NM-AIST.

A special appreciation goes to my supervisors; Prof. Karoli N. Njau and Prof. Chicgoua Noubactep, who, for the first time have successfully explored my research and academic potential as well as exposed me to all sorts of academia for society and industry. Dr. Kim Ho-Jin and Prof. Sung-Hoon Ahn are also acknowledged for their study materials characterization assistance from the Innovative Design and Integrated Manufacturing Laboratory, Department of Mechanical Engineering, Seoul National University

I extend many thanks to the NM-AIST academic staff for their remarkable theoretical and practical studies assistance. My kind-hearted thanks are further given to the African Development Bank (AfDB) Scholarship with grant number 2100155032816 through its NM-AIST based humble staff, i.e., Mr. Julius Msuri Lenguyana (Project Coordinator) and Ms. Victoria Ndossi (Project Administrator).

DEDICATION

I dedicate this work to researchers utilizing Metallic Iron-based materials for environmental remediation, specifically Prof. Chicgoua Noubactep, for keeping it up to date with studies in affordable water treatments for developing countries.

TABLE OF CONTENTS

LIST OF TABLES

LIST OF FIGURES

LIST OF APPENDICES

LIST OF ABBREVIATIONS AND SYMBOLS

AA	Activated Alumina
APHA	American Public Health Association
BC	Bone Char
Cl^-	Chloride
DW	Distilled Water
EDS	Energy Dispersive X-Ray Spectroscopy
EDTA	Ethylene Diamine Tetra-Acetic Acid
F^-	Fluoride
Fe^0	Metallic Iron
FeCPs	Iron Corrosion Products
FESEM	Field Emission Scanning Electronic Microscopy
GI	Granular Iron
HCO_3^-	Bicarbonate
HO^-	Hydroxide Ion
ICOH	Centre for Oral Health
ICOH	Inter-country Centre for Oral Health
ICP	Inductively Coupled Plasma
KF	Potassium Fluoride
KH_2PO_4	Potassium Dihydrogen Phosphate,
KNO_3	Potassium Nitrate
K_{sp}	Solubility-Product Constants
Na_2SO_4	Sodium Sulphate
NaCl)	Sodium Chloride
NaHCO3	Sodium Bicarbonate
NDRS	Ngurdoto Defluoridation Research Station
nZVI	Nanoscale Metallic Iron
Phen	1,10-Phenanthroline

SW or Fe^0 SW	Steel Wool
TDS	Total Dissolved Solids
TISAB	Total Ionic Strength Adjustment Buffer
UNICEF	United Nations Children's Fund
UV	Ultraviolet Light
UV/VIS	Ultraviolet/Visible Light
V_{iron}	Volume of the Initial Metallic Iron
V_{oxide}	Volume of Oxide
WHO	World Health Organization
WRC	Water Research Commission Report
XPS	X-Ray Photoelectron Spectroscopy
ZVI	Zero-valent Iron

CHAPTER ONE

INTRODUCTION

1.1 Background of the Problem

1.1.1 Overview over the Sources of Water and their Quality

The need for water by humans is essential for drinking, cooking, personal hygiene, cleaning, and sanitation systems. Only the fraction used for drinking and cooking should have safe drinking water quality. According to the World Health Organization (WHO), this represents just 15 L/person/day (Howard *et al.*, 2020). There are three primary sources of water: Rainwater, surface water, and groundwater. As a rule, typical rainwater is void of inorganic pollutants (As, F, Fe, U) but may be charged with pathogens and traces of organic pollutants (including humic substances). Surface water may be charged with both inorganic and ants but is certainly charged with pathogens (Hussam, 2009). The current paradigm prefers groundwater at great depth (boreholes better than shallow wells) as a source of drinking because it is generally free from pathogenic contamination. The arsenic crisis in Southeast Asia has demonstrated that groundwater may contain other undesirable pollutants (Hussam, 2009).

Most of the water used for domestic, commercial or industrial applications is treated to safe drinking water quality, whether it originates from rain, surface water or groundwater. Therefore, the safe drinking water supply can be significantly lowered if consideration is given to just the water needed for drinking and cooking. In rural areas where springs cannot deliver sufficient volumes of water to cover the annual need, groundwater is abstracted from shallow wells and boreholes. This trend is progressively replacing rainwater harvesting because of the reliability of groundwater. Again, if any pollutants are available in the soil matrix, there is a danger to exposing populations to another significant health problem due to contaminants such as fluoride and arsenic besides the pathogen contamination (Hussam, 2009).

Fluoride is a chemical pollutant in all-natural waters, including precipitation (Bjorvatn & Bårdsen, 1998) but commonly found in the earth’s crust (Manahan, 1994). Fluoride at high concentrations occurs in different areas worldwide and threatens public health and well-being (United Nations Children's Fund [UNICEF], 1999). Figure 1 shows the distribution of fluoride

throughout the world; coloured regions in the map are areas where water has elevated fluoride levels which directly relate to fluorosis.

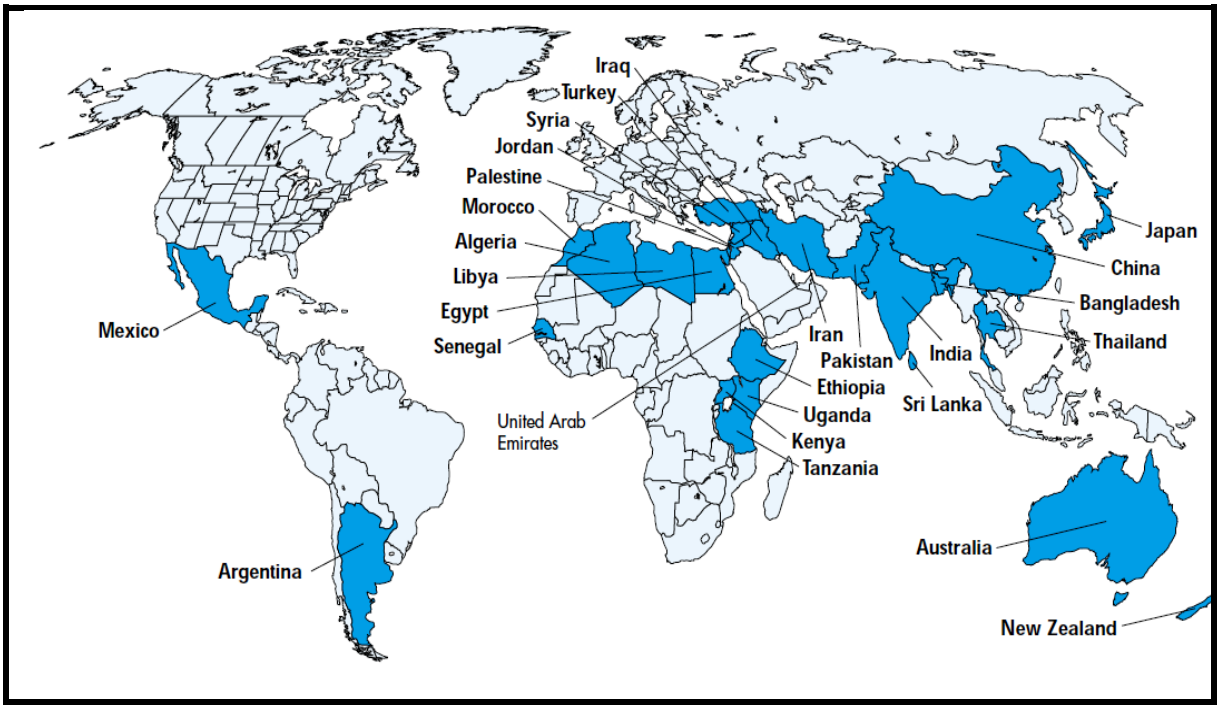

Figure 1: Countries with endemic fluorosis due to excess fluoride in drinking water (UNICEF, 1999)

Fluoride is a necessary constituent for humans and animals based on the total quantity uptake and its concentration in drinking water. Fluoride, at a low level, is universally recognized as an essential element to strengthen teeth; thus, preventing dental caries requires the addition of a limited fluoride amount to fluoride-free drinking waters. On the other hand, high levels of fluoride exposure present dental and skeletal fluorosis, this chronic disease is marked by mottling of teeth, softening of bones and neurological damage (Water Research Commission Report [WRC], 2004).

1.1.2 Chemistry and Geochemistry of Fluoride

The fluoride (F^-) is highly reactive due to being the most electronegative with a 3.98 value on the Pauling Scale (Pauling, 1960). Fluorine atom and molecular fluorine, F_2, never exist in nature, as contrasted by very soluble and stable fluoride (Hem, 1989; Brunt *et al.*, 2004; Ramadan & Hilmi, 2014; Jadhav, 2014). Fluorine is abundant in the earth crust and is the 13th most naturally occurring mineral (Harrison *et al.*, 1986); primary sources are minerals grouped into phosphates, fluorides, mica, and silicates (Teotia *et al.*, 1981). Water, food, air,

medicaments, and cosmetics are vivid fluoride entrance routes to the human body (Ayoob & Gupta, 2006; Jagtap *et al.*, 2012; Dahi, 2013), other sources include fluorotic industrial effluents, and windblown as well as rain splashed soil with high fluoride content (Ranjan, 2015). Since fluoride in water contributes about 60 % of noted fluorosis (Jagtap *et al.*, 2012) and high fluoride concentrations in drinking water is of great importance as a source of fluoride (WHO, 2011) therefore, this study considers water as a major source of fluoride for discussion.

Most surface water sources are less over-fluoridated compared to groundwater unless there are significant interactions with minerals bearing high fluorotic rocks as in some cases of groundwater. Virtually, water is observed to be balanced by a hydrologic cycle, where precipitation get enriched with carbon dioxide ($CO_{2)}$ in: (a) The atmosphere as precipitation falls, (b) From the soil air during precipitation percolation, and (c) Microbial activities within the precipitation moistened soil (Ayoob & Gupta, 2006; Malango *et al.*, 2017). The net effect of dissolved CO_2 is to enhance hydrogen ions (H^+) concentration in groundwater (Equations 2 and 3), and subsequent weathering of interacting minerals (Handa, 1975; Frencken, 1992) by Congruent (Equation 4) or Incongruent (Equation 5) means (Lottermoser, 2003).

$$CO_{2(g)} + H_2O_{(l)} \Leftrightarrow H_2CO_{3(aq)} \quad (1)$$

$$H_2CO_{3(aq)} \Leftrightarrow H^+_{(aq)} + HCO_3^-{}_{(aq)} \quad (2)$$

$$HCO_3^-{}_{(aq)} \Leftrightarrow H^+_{(aq)} + CO^-_{3(aq)} \quad (3)$$

$$MeAlSiO_{4(s)} + H^+_{(aq)} + 3H_2O_{(l)} \Rightarrow Me^{x+}_{(aq)} + Al^{3+}_{(aq)} + H_4SiO_{4(aq)} + 3OH^-_{(aq)} \quad (4)$$

$$2MeAlSiO_{4(s)} + 2H^+_{(aq)} + H_2O_{(l)} \Rightarrow Me^{x+}_{(aq)} + Al_2Si_2O_5\,(OH)_{4(s)} \quad (5)$$

Where, Me = Ca, Na, K, Mg, Mn or Fe; x = Me charge

The solubility of fluoride in groundwater varies with the variation of fluoride bearing rocks, e.g. fluorite and cryolite minerals are sparingly soluble in water under normal temperature and pressure (Saxena & Ahmed, 2001; 2003; Zhu *et al.*, 2015). Apart from adsorption, desorption, residence time, water-rock interaction and precipitation reactions being essential factors on fluoride release and capture processes, the basic concerning fluoride release in water strictly

depends on dissolution activity of fluoride minerals compared to the availability of fluoride bearing minerals in rocks (Malago *et al.,* 2017). Acidity in water tends to favour fluoride adsorption on rock minerals as contrasted by alkaline conditions that usually enhance fluoride dissolution into water (Borgnino *et al.,* 2013). Alkaline environments prevail in volcanic areas and are mostly associated with HCO_3^- species (Kitalika *et al.,* 2018) which enhances fluoride dissolution activity while precipitating carbonates with associated minerals, e.g. fluorite (Equation 6).

$$CaF_{2\,(s)} + 2HCO_{3\,(aq)}^{-} \Rightarrow CaCO_{3\,(s)} + 2F_{(aq)}^{-} + H_2O_{(l)} + CO_{2\,(g)} \quad (6)$$

$$K_{sp} \text{ for } CaF_2 \Rightarrow 3.45 \times 10^{-11} \quad (7)$$

$$K_{sp} \text{ for } CaCO_{3(s)} = 3.36 \times 10^{-9} \quad (8)$$

Equation (6) is said to mostly determine the concentration of fluoride in natural waters (Ayoob & Gupta, 2006) except for a high calcium environment above fluorite solubility limit due to the common ion effect (Apambire *et al.,* 1997). Solubility-product constants (K_{sp}) values for compounds at 25 ^{0}C (Equations 7 and 8) are evident on relatively low solubility of CaF_2; thus, calcium will immobilize fluoride from water to a great extent. The observation is also conversant with most highly reported fluorotic waters being of less or with no calcium content (Simon *et al.,* 2016) and state of the art application of the same approach in different calcium-based defluoridation techniques (Nath & Dutta, 2015).

The blessing of calcium to render fluoride availability has a limited potentiality to highly fluoridated water as excess fluoride remains free if not acted by other means or chemicals (e.g. Magnesium to a reasonable concentration) (Ali *et al.,* 2016). This interaction is also a curse to animals as their bones are composed of accessible calcium by fluoride. Water with high fluoride has negative impacts on plants and animals. In particular, animals have been suffering from visible effects such as dental and skeletal fluorosis (Jolly *et al.,* 1968) concerning fluoride concentrations in water, as indicated in Table 1. Fluoride (F^-) is analogous to hydroxide ion (HO^-) in size and charge (Heimann *et al.,* 2018b). Consequently, because of its strong electronegativity, F- readily replaces it in the soft Hydroxyl apatite compound composing bones and teeth and forms hard fluorapatite compound (Equation 9), resulting in fluorosis (Kut *et al.,* 2016).

$$Ca_5(PO4)_3OH_{(s)} + F^-_{(aq)} \Rightarrow Ca_5(PO4)_3F_{(s)} + OH^-_{(aq)} \quad (9)$$

Table 1: Fluoride concentrations and their health effects

Fluoride (mg/L)	Potential health effects
<0.1	High levels of dental decay
0.1-1.5	Beneficial effects in preventing dental caries
1.5-3	Dental fluorosis
3–6	Dental and skeletal fluorosis
>10	Crippling fluorosis

WHO (2006 & 2011)

1.2 Statement of the Problem

Metallic iron (Fe^0) materials facilitate safe drinking water provision; several contaminants such as arsenic and microbes successfully combated (Makota *et al.,* 2017). Fluoride is yet to be declared safe from drinking water using Fe^0 (Ndé-Tchoupé *et al.,* 2015; Heimann, 2018; Heimann *et al.,* 2018). Few studies have been done on defluoridation using metallic iron, and the existence of co-solutes such as chlorides and bicarbonates seems to inhibit efficiency (Antia, 2015). This study intends to exploit further the behaviour and use of filamentous Fe^0 materials (steel wool or Fe^0 SW), being efficient than courser (large-sized) ones (Mwakabona *et al.,* 2017).

1.3 Rationale of the Study

Metallic iron operates by its corrosion products that possess the ability to present adsorption (for anionic contaminants), co-precipitation, and size exclusion effects (Noubatep, 2010; Noubactep, 2011; Ndé-Tchoupé *et al.,* 2015). The existence of co-solutes such as chlorides and bicarbonates seems to alter the formation of these corrosion products and competes for adsorption respectively, at controlled study conditions (Martínez-Miranda *et al.,* 2011; García-Sánchez *et al.,* 2013; Megha & Meera, 2016). These are collectively known to diminish the quantitative removal of fluoride from water; however, considering many operation factors is essential before declaring such limitation, especially when it comes to real-life application. Hence, a need for an in-depth study and use of porous metallic iron with consideration of multiple operational conditions is required.

1.4 Research Objectives

1.4.1 General Objective

Investigation of the suitability of Fe^0 for water defluoridation using laboratory-scale batch systems.

1.4.2 Specific Objectives

(i) To characterize the suitability of steel wool (Fe^0 SW) as reactive material for water defluoridation.

(ii) To perform batch defluoridation studies in laboratory synthetic water using Fe^0 SW.

(iii) To propose optimized conditions for water defluoridation, preferably at large scale fieldwork.

1.5 Research Questions

Questions considered in this study were:

(i) Which locally available Fe^0 SW materials are suitable for fluoride removal?

(ii) How to reduce high fluoride content to acceptable levels?

(iii) How would field water treatments, using Fe^0 perform?

1.6 Significance of the Research

Following critical studies on Fe^0 SW as a water treatment agent, in a particular time under natural environmental condition simulations; then drinking water containing elevated amounts of fluoride can be treated at an affordable cost with this convenient and straightforward technology.

1.7 Delineation of the Study

The study intends to use suitably characterized SW as a source of Fe^0 that will be responsible for fluoride removal in the aqueous setting. The Fe^0 SW will be subjected to in batch studies, thereby by providing an aqueous iron condition that will immediately generate corrosion and

associated products responsible for water defluoridation. Synthetic water to be treated will contain respective co-solute contaminants that simulate natural water major compositions and allowed to equilibrate over desirable time before assessment of final water quality.

CHAPTER TWO

LITERATURE REVIEW

2.1 Affordable Defluoridation Techniques

2.1.1 Coagulation

Aqueous F^- is: (a) Very stable and has (b) A small size (Moussa *et al.,* 2017). Generally, such colloidal (negatively charged) species mutually repel each other in the aqueous phase. Thus, by adding a coagulant (metallic salts or polymers) with an opposite charge to the F^- polluted water, the neutralization of the repulsive charge and "destabilization" of F^- species could be easily achieved. Here, Van der Waals forces could cause them to agglomerate and form micro floc to ease their removal from water (Vardhan & Karthkeyan, 2011; Mwakabona *et al.,* 2014; Dahi, 2016). Thus, it corresponds to the principle of the coagulation-flocculation process. The main factors influencing the effectiveness of this process include among others: (a) The initial pH of the water to be treated, and (b) The dose, mass and type of the used coagulant. An example of tested polymers is the Moringa seed extract, which with an optimal dose of 1000 mg/L. Moringa seed extract, was reported to be efficient at quantitatively removing F- (75 % at pH 3 and up to 86 % at pH 6) from the water with an initially F- concentration of 5 mg/L (Vardhan & Karthkeyan, 2011; Mwakabona *et al.,* 2014). Unfortunately, this approach required a very elevated amount of the coagulant with a pre- or post-adjustment of the pH value. On the other hand, the use of metallic salts as a potential source of cationic coagulants has also endeavoured because not only do: (a) Metallic ions such as Fe^{2+}/Fe^{3+}, Ca^{2+}, Mg^{2+} and Al^{3+} preferentially bind with F- in water (Shriver *et al.,* 1994) but (b) They also form insoluble compounds with it (Sharpe, 1992). A well-known case involved the use of Al^{3+} (the Nalgonda technique).

(i) The Nalgonda Technique

The Nalgonda technique for water defluoridation, as tested for the first time in Tanzania in 1990 in Ngurdoto, Arusha, was developed in India during the early 1970s (Dahi *et al.,* 1996; Modi & Soni, 2013; Dahi, 2016). The approach of the technique relies on three primary operations: Coagulation and sedimentation. Alum in treatment serves a coagulant role for F^- in the water and subsequent addition of lime as flocculent (Indian Standard, 1989; Mwakabona *et al.,* 2014). Alum hydrolyzes once in the water and forms Polyhydroxy-aluminum complexes, the polymeric compounds responsible for trapping F- and ease its sedimentation (Mwakabona *et*

al., 2014). Aqueous F- is therefore believed to be removed here via a co-precipitation process. Upon proper design, household filters based on the principle of the Nalgonda technique were reported capable of addressing the problem in Ngurdoto. More importantly, the filters were affordable to the low-income populations of this locality (Dahi, 2016).

The effectiveness of the Nalgonda technique was, in reality, not satisfactory in Tanzania as it was in India (Dahi *et al.,* 1996; Mjengera & Kongo, 2003; Tewari & Dubey, 2009; Shrivastava & Vani, 2009; Modi & Soni, 2013; Mwakabona *et al.,* 2014). The 800 mg/L alum and 80 mg/L lime needed for the operation could reduce the F^- concentration (22 mg/L) of the Tanzanian polluted water to 3.5 mg/L (Dahi *et al.,* 1996, Mwakabona *et al.,* 2014, Dahi, 2016). In other words, this was not low enough to the permissible level of 1.5 mg/L set by the WHO, even though it served the 8.0 mg/L and 4.0 mg/L Tanzania guideline at that time. Unfortunately, more alum and lime were required to achieve desirable guidelines for drinking conformity. There is even another important issue about this technique that discredits it. According to a report by Meenakishi and Maheshwari (2006) reiterated by Modi and Soni (2013) using alums for water defluoridation leads to the in-situ formation of toxic fluoro-alumino complexes known for causing the very dreaded Alzheimer's disease. It means that in trying to solve this problem, this technique could finally create another serious one.

2.1.2 Adsorption

(i) Metal Oxides and Hydroxides

Studies show recent testing of metals oxides, hydroxides, and natural rocks for aqueous F^- removal in Tanzania (Mwakabona *et al.,* 2014). As an example, natural locally available aluminium ore (bauxite) has either been directly used because of its reported good fluoride adsorption capacity (Sajidu *et al.,* 2008) or activated alumina (AA) synthesized from it and tested (Veressinina *et al.,* 2001; Renuka & Pushpanjali, 2013). The porous nature of AA makes it a versatile adsorptive material. The AA's characteristic surface charge property arises from surface hydroxyl groups (Goldberg *et al.,* 1996; Mulugeta *et al.,* 2015). Unlike neutral pH conditions, the surface of AA is more positive at pH values below 6.0 that exhibits substantial fluoride adsorption features. In the neutral pH range, the affinity of the AA surface for fluoride is much lower (Renuka & Pushpanjali, 2013; Ndé-Tchoupé *et al.,* 2015). Typical pre-adjustment

of pH in polluted water is then required as long as AA is to perform efficiently. It could invariably mean a post-treatment pH to meet desirable drinking water guidelines.

The main problem with using AA is that desorption of adsorbed fluoride occurs once the material is saturated (Veressinina *et al.,* 2001; Renuka & Pushpanjali, 2013; Mwakabona *et al.,* 2014). Besides this, AA manufacturing involves calcination (at about 500°C) of bauxite. In order words, it is not a readily available material and hence not easily affordable for low-income populations. The direct use of the local bauxite is also not suitable as instead of only treating the water, it could itself be another source of contamination.

(ii) Bone Char

The utilization of charcoal obtained by calcination of animal bones (bone char) under well-controlled conditions (temperature and duration) for water defluoridation is an old practice (Fawell *et al.,* 2006; Dahi, 2016). Its suitability has been widely tested and is well documented (Dahi *et al.,* 1996; Makwabona *et al.,* 2014; Ndé-Tchoupé *et al.,* 2015; Dahi, 2016). The maximum defluoridation capacity of bone char (BC) reaches 60 % even at neutral pH (Renuka & Pushpanjali, 2013). The first applications of the BC technique must have occurred during the early 1940s in the USA (Fawell *et al.,* 2006; Dahi, 2016). Because BC: (a) Is available from waste bones, e.g. at abattoirs, (b) Could easily be made and meet local requirements, (c) Can be thermally regenerated, and (d) Is relatively cheap, the BC technique is at present considered the most efficient and affordable technique for F- removal (Mjengera & Nkongo, 2003; Murutu *et al.,* 2012; Rojas-Mayorga *et al.,* 2013, 2015). It can account for why the Thailand Inter-country Centre for Oral Health (ICOH) has, together with the WHO, been strongly advocating it as an appropriate technique for household use during these recent years (Dahi, 2016).

The mechanisms and kinetics by which F- is removed by BC have been subject to comprehensive investigations (Bregnhøj & Dahi, 1997; Bregnhøj *et al.,* 1997; Tovar-Gómez *et al.,* 2013; Rojas-Mayorga *et al.,* 2015; Kariuki *et al.,* 2015). The BC is predominantly made up of hydroxyapatite [$Ca_{10}(PO_4)_6(OH)_2$] (Davey, 1939; Fawell *et al.,* 2006; Hassan *et al.,* 2008; Gwala *et al.,* 2014). Hence, aqueous F^- is captured and removed by BC through chemisorption and ion exchange between F and the hydroxyapatite hydroxyl function, which leads to the formation of fluorapatite [$Ca_{10}(PO_4)_6F_2$] (McCann, 1953; Kaseva, 2006; Makwabona *et al.,* 2014). Electrostatic attraction of dissolved F^- is also known to occur in parallel with F^-adsorbed

via physisorption (Ndé-Tchoupé *et al.,* 2015); nevertheless, the kinetics of hydroxyapatite dissolution certainly limits the extent of ion exchange.

This solid background has facilitated the rational design and field testing of the BC technique in the Kitefu village in Tanzania (Mosha *et al.,* 1996). The creation of the Ngurdoto Defluoridation Research Station (NDRS) by the Tanzanian ministry of water appears as the most significant evidence for the country's growing interest in the technique (Mjengera & Nkongo, 2003; Mwakabona *et al.,* 2014). Dahi (2016) reported the existence of some thirty defluoridation units, very similar to the ICOH defluoridator, which have been installed at the Kitefu households even though operating with a questionable removal capacity.

Despite a well-demonstrated efficiency, the effective field application of the BC technique is still severely confined by the two main issues. These are: (a) The belief that the material could harbour bacteria (Renuka & Pushpanjali, 2013), and (b) The unavailability of a good quality BC at the local level, which have so far been the main reason for unsatisfactory and frustrating results (Fawell *et al.,* 2006; Makwabona *et al.,* 2014). The production of a good quality BC (meaning with a high defluoridation capacity) requires preparations under several specific conditions (e.g., controlled temperature and O_2 level for a fixed duration) (Puangpinyo & Osiriphan, 1997). Therefore, it certainly demands some training and the utilization of appropriate tools. In other words, only commercially distributed BC could be reliable for communities like Kitefu village in Tanzanian. Nevertheless, this is, unfortunately, unavailable (Jacobsen & Dahi, 1997). It shows that the problems associated with the BC technique pose a severe threat to its effective application hence its acceptability.

(iii) Activated Plant Charcoal

The limitations associated with the BC techniques have motivated the development of activated plant charcoal as a viable alternative (Makwabona *et al.,* 2014). Activated carbon or activated charcoal is prepared from plant biomass by heating (as required in the manufacturing of BC, alumina and the like) at a temperature that is necessary to render it porous (Mohammad-Khah & Ansari, 2009). Aqueous F^- is believed to be removed via adsorption occurring both in the pores and at the surface of the activated carbon (Hanumantharao *et al.,* 2004). The fluoride removal capacity of activated carbon of this type depends more on the nature and the origin of the plant used for its manufacturing than the preparation and operation conditions (Janaradhan

et al., 2007; Chakrapani *et al.,* 2010). For example, investigating the fluoride removal efficiency of citrus three different plant species peels activated carbon prepared at the same preparation condition, Chakrapani *et al.* (2010) observed significant differences among their efficiencies. However, regardless of the nature and the origin of the plant used for its preparation, the performance of the filter material is pH-dependent (Kadirvelu *et al.,* 2000). High fluoride removal capacities were at lower pH values (Tembukhar & Dongre, 2006; Chakrabarty & Sarma, 2012), and thus implying the necessity of a pH pre-adjustment of the water to be treated in many cases.

Again, pre-and post-treatment pH regulations of water are also a limitation here. Moreover, a complicated issue to solve will be identifying a plant (abundantly available in all needed areas) that could be used to prepare activated charcoal that treats fluoride polluted waters with the same efficiency and satisfactorily.

(iv) Biomaterials

The limitations of the previous techniques have forced scientists during these recent years to initiate numerous studies aiming at finding a workable way in Tanzania for local exploitation of available biomaterials for the preparation of defluoridation media. The introduction of secondary contaminants to treated water due to leaching and regeneration difficulties were reviewed to be disadvantages of biomaterial (Kamathi, 2017) and hence required modifications which later proved successful in decontamination of other pollutants. Wagutu *et al.* (2018) demonstrated the suitability of Biogenic chitosan-hydroxyapatite composite to field water defluoridation; the main challenge was the applicability of adsorption at low pH as it required water pre-acidification.

2.2 Characterization of Metallic Iron Materials

Characterization aims at identifying a relationship between the structure of the material and associated properties or application (Fahlman, 2007); approaches used may include one or a combination of chemical, physical, mechanical, optical and thermal treatments (Park & Lakes, 2007). The use of metallicc iron (Fe^0) in environmental treatment and remediation (Zou *et al.,* 2016) and many characterization protocols have been reviewed accordingly (Li *et al.,* 2019). Depending on whether nano, micro and or macro-ZVI characterized materials, chemical characterization by using dilute Ethylene diamine tetra-acetic acid (EDTA) solution was found

to be the simple and most affordable tool for macro-ZVI materials (Hildebrant, 2018; Hildebrant *et al.*, 2019; Hu *et al.*, 2019; Naseri *et al.*, 2017; Noubactep *et al.*, 2005; Noubactep *et al.*, 2004) such as iron scraps, nails, granular iron materials and steel wool. However, EDTA has been identified to hinder the availability of complexed iron during Spectrophotometric determination by 1,10-phenanthroline (Phen) (Oviedo & Rodríguez, 2003; Monsen & Page, 1978; Walmsley *et al.*, 1992); thus, an additional procedure is necessary for EDTA-iron de-complexation. Consequently, to avoid any supplementary procedures that are time-consuming and relative cost, direct use of Phen in-place of dilute EDTA solution during characterization is suggested.

The Phen is considered a versatile ligand (Sammes & Yahioglu, 1994), where chelate formation as one of its diverse application has become a significant branch of science (Brandt *et al.*, 1954). The use of Phen in spectrophotometric studies is valid as several metals are capable of forming complexes associated with colour reactions (Lazić *et al.*, 2010). Ferrous iron (Fe^{2+}) forms an orange-red complex with three molecules of Phen (Equation 10), the colour intensity is directly proportional to Fe^{2+} concentration which obeys beer's law (American Public Health Association [APHA], 2005) and its variations exhibit linearity with time (Equation 11). Similar applications such as the elimination of metallic interference by Phen reagents are remarkable (De-Doncker *et al.*, 1985; APHA, 2005).

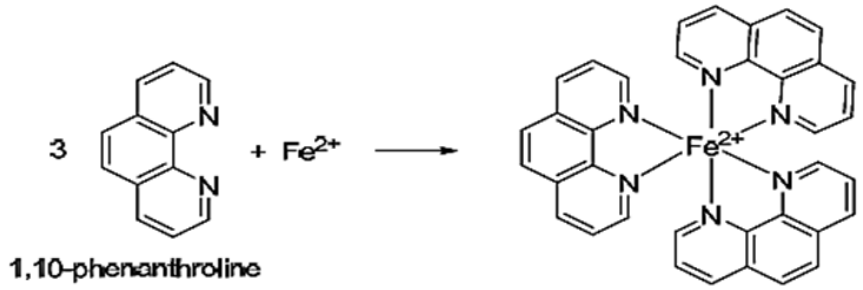

(10)

$$[Fe]_t = (k_{Phen})t + b \quad (11)$$

The suitability of Phen arises from its Fe^{2+} chelate stability. Colour standards are stable for at least six (6) months and are unaffected on protracted UV light exposure (Fortune & Mellon, 1938; Schilt, 2013; APHA, 2005) as contrasted by EDTA-Iron complexes that are susceptible to photo-degradation (Pietsch *et al.*, 1996). Moreover, the colour formed is pH-independent from 3 to 9 (APHA, 2005) but rapid colour development is at pH values of 3.5±0.6 unit (APHA, 2005; Lazić *et al.*, 2010). Availability of other metals capable of forming stronger Phen complexes was observed to be a major interference (Lazić *et al.*, 2010; Analytical Methods

Committee, 1978), but only an excess of Phen reagent was required to diminish their effects before Fe^{2+} complexation (APHA, 2005). Unlike EDTA which favours stable complex formation with ferric iron (Fe^{3+}) species (Harris, 1991), Phen forms stable complexes with the direct colour-forming Fe^{2+} species (Rizvi, 2015) that are 10^5 stronger than their Fe^{3+} complexes counterparts (Ibanez *et al.,* 1988). The Fe^{2+} complexes of EDTA are much stronger reluctant (Joseph *et al.,* 1996; Mazur, 1961) that accelerates the dissolution of ZVI under characterization, a situation deceptive to field condition certainty; hence direct use of Phen chelate have an added advantage on becoming the simple and most affordable ZVI characterization method.

2.3 Defluoridation by Metallic Iron

2.3.1 State of the Art Defluoridation by Metallic Iron

Filters incorporating metallic iron (Fe^0) have been confirmed to be capable of solving different types of pollutants (biological and chemical) in water (Noubactep, 2011). The Fe^0 materials are capable of removing many contaminants because, in aqueous solution, they produce solid iron (hydr)oxide corrosion products which are highly effective contaminant-scavenging agents for anions (Noubactep *et al.,* 2012; Phukan, 2015).

The Fe^0/water system also demonstrates that; Fe^0 oxidative dissolution (Equation 12) and the precipitation of its oxide-hydroxides (Equation 13) occur in the presence of contaminants (Ndé-Tchoupé *et al.,* 2015), thereby making complex interactions among dissolved species, Fe^0, its oxide-hydroxides and intermediate species (Crawford *et al.,* 1993). The Fe^{2+} and H/H_2 are intermediate species which presents reducing properties, with increased strength upon adsorption onto (nascent) oxides (White & Peterson, 1996).

$$Fe^0 + 2H^+ \Rightarrow Fe^{2+} + H_2 \quad (12)$$

$$Fe^{2+} + 2OH^- \Rightarrow Fe(OH)_2 \quad (13)$$

Fallacies regarding Fe^0 as a sole reducing agent arises due to the complexity of processes in Fe^0/H_2O systems, and it could give reasons to limited defluoridation studies using Fe^0 (Henderson & Demond, 2007; Obiri-Nyarko *et al.,* 2014; Noubactep, 2017). The standard electrode potentials for fluoride (E^0 = 2.87 V, Equation 14) and Fe^0 (E^0 = 0.44 V, Equation 15)

indicate that Fe^0, in theory, is unable to reduce F, i.e., F_2 would oxidize Fe^0 (Ndé-Tchoupé *et al.,* 2015).

$$2F^- \Rightarrow F_2 + 2e^- \quad (14)$$

$$Fe^0 \Rightarrow Fe^{2+} + 2e^- \quad (15)$$

Thus contaminant removal is based on the Fe^0 corrosion pathways, which are: (a) The volume of each oxide (V_{oxide}) is larger than the volume of the initial metallic iron (V_{iron}), and (b) During the precipitation of oxides, contaminants can become trapped (Crawford *et al.,* 1993).

Pure physical sequestration may occur independently of the Fe (hydr)oxide adsorptive affinity (Duff *et al.,* 2002). However, pollutant removal by size exclusion improve with the filter service life, i.e., $V_{oxide} > V_{iron}$ (Pilling & Bedworth, 1923), regardless of any adsorptive affinity between oxides and pollutants (Ndé-Tchoupé *et al.,* 2015). Consequently, Fe^0/H_2O systems are commonly appropriate for removal of anionic pollutant species but are also suitable or applicable towards other species removal (Tepong-Tsindé *et al.,* 2015; Phukan, 2015).

Adsorption, co-precipitation, and size-exclusion are key features towards pollutant removal within reactive Fe^0/H_2O systems (Ndé-Tchoupé *et al.,* 2015; Naseri *et al.,* 2017). Due to successive generation of iron oxides in the system, filter efficiency depends on its physical design for accommodating significant intrinsic porosity; hence steel wool can serve the purpose (Naseri *et al.,* 2017).

2.3.2 Efforts to Date

(i) Nanoscale Attempts

Fluoride removal in water has been widely addressed using nanoscale zero-valent iron (nZVI) materials. Jahin (2014) showed that to a 5 mg/L Fluoride contaminated solution; 85% defluoridation efficiency was achieved within 34 minutes from 0.6 g/L nZVI dosage at pH 4. Raul *et al*. (2012) revealed that, to a 15 mg/L fluoride solution, more than 70% removal efficiency was noted using 1 g/L nZVI dosage for 3 hours contact time. In the presence of interfering co-solutes, Liu *et al.* (2016) reported fluoride removal efficiency from 76% to 100% when equilibrated with 25 mg/L fluoride contaminant in 0.05 g nZVI adsorbent within 8 hours. Generally, nZVI is an ideal efficient material due to their excellent shorter remediation durations and low adsorbent dose requirements (Dhillon & Kumar, 2019). As a rule, nZVI has got their

setbacks when considered for field applications (Parashar *et al.,* 2019); this includes: (a) Diminished adsorptive capacity due to agglomeration in aqueous remediation, and (b) Their minimal size allows quickly clogging of filters and results in reduced pressures.

(ii) Conventional Iron Aqueous Systems

Excellent efforts are addressed on course iron materials for water treatments (Noubactep, 2010, 2013, 2017, 2018; Naseri *et al.,* 2017; Mwakabona *et al.,* 2017); they serve majority in developing countries at individual and community level. Thus, they facilitate independent manipulation and implementation of simplified water treatment processes for safe water provision. Accordingly, a presented concept that utilizes metallic iron (Steel wool) based filters as one of decentralized technology for fluoride removal in water exist (Ndé-Tchoupé *et al.,* 2015); it centres on an in-situ generation of iron corrosion products (FeCPs) where contaminants removal is by co-precipitation, adsorption and size exclusion. At first, Heimann *et al.* (2018a) used column studies to test the concept validity under consideration of Chloride (Cl^-) and Bicarbonate (HCO_3^-) co-solute contaminants where they concluded that defluoridation by Fe^0 is possible; but quantitative removal of aqueous fluoride is significantly affected by the existence of such co-solutes in the order of $Cl^- > HCO_3^-$, hence in-situ concept practicability should be reconsidered. Later on, experiments revealed the feasibility of this concept to be valid but with a conclusion on difficultness to remove high aqueous fluoride contents due to high quantity demand of iron materials and or thicker filter layers requirements (Heimann *et al.,* 2018b). Furthermore, conventional Fe/H_2O system was verified to be of ion-selective in nature using dye flushing studies (Btatkeu-K *et al.,* 2016; Heimann *et al.,* 2018b) that confirmed the relative observed low defluoridation efficiency. Ndé-Tchoupé *et al.* (2019a) realized a comparative batch study using SW and granular iron (GI) materials after pre-corrosion for 46 days and subsequent equilibration with fluoride contaminants for 30 days. In their research, SW showed better performances compared to GI. However, overall findings enabled them to conclude that conventional metallic iron is not suitable for quantitative aqueous fluoride removal; and propagation of their earlier proposed concept should, therefore, be avoided. On the other hand, and in addition to these observations, such researchers univocally declared that since aluminium alloys show better defluoridation efficiencies, then aluminium-iron alloys are suggested as a way forward in water defluoridation research (Noubactep, 2018; Heimann *et al.,* 2018). Meanwhile, there is a provision of concurrent suggestion on the necessity of exploring alternative ways to avoid defluoridation using metallic iron (Ndé-Tchoupé *et al.,* 2019a), e.g.

using Rainwater harvesting and blending practices (Marwa *et al.*, 2018; Ndé-Tchoupé *et al.*, 2019b).

Based on current observation, and the fact that metallic iron nanomaterials perform better in water defluoridation, this study aims at a further critical assessment of metallic iron suitability as defluoridation agent using temporal environmental corrosion conditions based on the proposed concept. Preference of steel wool is due to their large surface area compared to courser iron-bearing materials, e.g. scraps, nails, and GI; hence physicochemical reactions and changes responsible for fluoride remediation should be realized here as all chemical reactions occur at a molecular level. Utilization of batch experiments enabled studying of contaminants in the reaction vessel and captured crucial remediation possibilities from none to full corrosion and rust developments.

CHAPTER THREE

MATERIALS AND METHODS

3.1 Characterization of Steel Wools

3.1.1 Solutions used for Characterization of Steel Wool

Preparation of working solutions consisted of a monohydrated 1,10-Phenanthroline (Phen) (Merk, Darmstadt, Germany) and a disodium salt of Ethylene diamine tetra acetic (Merk, Darmstadt, Germany). An iron standard solution (1000 mg L^{-1}, NIST) from Hach Company was used to calibrate the spectrophotometer. Other used chemicals included ascorbic acid, hydrochloric acid, and nitric acid. All used chemicals were of analytical grade.

3.1.2 Metallic Iron Materials used for Characterization of Steel Wool

A total of nine (9) used commercial steel wool (Fe^0 SW) specimens, SW1 to SW 8 imported from China, and SW9 were locally purchased from East Africa Steel Wool (Ind.) Limited in Dar Es Salaam (Tanzania). Tested nine Fe^0 SW covered all grades of steel wools. Table 1 summarizes the characteristics of iron materials and their elemental composition.

3.1.3 Experimental Procedures for Characterization of Steel Wool

(i) Elemental Composition of used Metallic Iron Steel Wool

The present study adopted the experimental procedure reported by Sakai (2015), where the working solution contained HNO_3 (70%), HCl (35%) and de-ionized water at a 1:1:1 ratio by volume. Analytes preparation involved the addition of 12 mL of the mixed acid solution to 0.5 g of Fe^0 SW in a glass beaker. Gradual heating of analyte solution to 200 ^{0}C for 30 minutes followed after 10 minutes pre-digestion time lapse at room temperature (23±2 ^{0}C) under a watch glass cover. After 15 minutes of analyte solution cooling, de-ionized water was reconstituted to 100 mL for analysis. Then, 1 mL of the sample was diluted with de-ionized water to a mark in a 250 mL volumetric flask prior to Inductively Coupled Plasma (ICP) analysis.

(ii) Iron Dissolution

Ethylene Diamine Tetra Acetic Acid vs 1,10 Phenanthroline under Varied Conditions

Iron dissolution studies used 0.01 g of each Fe^0 material in 50 mL of 2 mM Phen, 6 mM Phen and 2 mM EDTA solutions for four (4) days using 50 mL CellStar to hold solutions under closed experimental systems. It involved two designed sets whereby one was subjected to slight inversion prior sampling (which aided evenly mixing the sample before using it for analysis) and the other with no inversion while taking an aliquot. The experimental setup was modified from conventional Fe^0 Characterization protocols by EDTA under room temperature.

(iii) Characterization of all Steel Wool in Ethylene Diamine Tetra-Acetic Acid and 1,10-Phenanthroline

Intrinsic reactivities of all SW were assessed using 0.1g in 50 mL 2 mM EDTA and Phen. An experimental setup was adopted from conventional Fe^0 Characterization protocols by EDTA under room temperature.

3.1.4 Analytical Method for Determination of Total Iron

Determination of aqueous iron concentration involved a Rayleigh Ultraviolet/visible Spectrophotometer (UV/VIS Spectrophotometer) (Beijing Beifen-Ruili Analytical Instruments (Group) Co., Ltd), at a wavelength of 510 nm using a 1.0 cm cuvette. The calibrated instrument could detect the iron concentration of ≤ 10 mg L^{-1}. As discussed elsewhere, samples from the EDTA method were reduced to Fe (II) before complexation using ascorbic acid (Hu *et al.*, 2019).

3.1.5 Expression of Results

Dissolution kinetics of tested ZVI material was anticipated to follow linearity order (Equation 11). Regression parameters (k_{Phen}, R^2 and b) from experimental data allowed computation of the linear dissolution function of tested ZVI material. The R^2 values show a relationship of corrosion rate for each material through the extent of linearity. Noubactep *et al.* (2004), Noubactep *et al.* (2005), Noubactep *et al.* (2009), Btatkeu-K *et al.* (2013) and Hildebrant (2018) showed that direct assessment of the calculated rates of iron dissolution (k_{Phen}) could be used to indicate the dissolution efficiency of tested ZVI materials, while the calculated intercept ('b')

values could be used to indicate the relative amount of pre-existing corrosion products present on the material surfaces.

3.2 Synthetic Water Defluoridation at Laboratory Batch Studies

3.2.1 Solutions for Batch Defluoridation Experiments

(i) Working Solutions

Preparation of used 23±2.0 mg/L contaminants involved dilution of respective 1000 mg/L stock solutions, previously made using the corresponding weighed mass after drying in an oven at 105 ^{0}C to a constant weight. Fluoride (Potassium Fluoride, KF), Chloride (Sodium Chloride, NaCl), Sulphate (Sodium Sulphate, Na_2SO_4), Nitrate (Potassium Nitrate, KNO_3), Bicarbonate (Sodium Bicarbonate, $NaHCO_3$), and Phosphate (Potassium Dihydrogen Phosphate, KH_2PO_4). All chemicals used were analytical grade from Merc Manufacturers with an Assay range of 99-100%. Distilled water (DW) served in preparation of stock solutions and subsequent dilution reconstitutions; DW had an initial quality of Total Dissolved Solids (TDS) value of 1.06 mg/L and pH value of 7.08 at 25 ^{0}C. In addition to the control solution, DW; there were six (6) used different fluoride contaminated working solutions, namely: (a) Fluoride in DW (reference) solution, (b) Fluoride and Chloride in DW, (c) Fluoride and Sulphate in DW, (d) Fluoride and Nitrate in DW, (e) Fluoride and Bicarbonate in DW, and (f) Fluoride and Phosphate in DW.

(ii) Fluoride Buffer Solution

The Total Ionic Strength Adjustment Buffer (TISAB) solution was made following Rice *et al.* (2017).

3.2.2 Solid Materials

(i) Metallic Iron

Locally available Steel Wool, used as Fe^0 material, was purchased from East Africa Steel Wool (Ind.) Limited (Dar Es Salaam, Tanzania). The material is available as a fibrous sponge and was identified to possess a very fine quality category (A SHINETM Brand of Grade 00). Elemental composition elucidation of this material is available from tabulated section 3.1.3 (i) results. The material used received no pre-treatment.

3.2.3 Experimental Procedure and Analytical Method

(i) Investigation of all Steel Wool Batch Reactions for Defluoridation

Batch studies were carried out in plastic containers with an inner diameter of 3.5 cm and a height of 1.5 cm. The mass of Fe^0 varied at 0.1 g and 1.0 g with ±0.002 g uncertainty, followed by even distribution of weighed masses in their respective designated contaminant plastic containers. Different fluoride-contaminated working solutions had adjustments into initial pH categories of 2.5 unit intervals (i.e., pH 4.5, 7.0 and 9.5, with ±0.1 unit uncertainty) using dilute acetic acid and ammonia solutions each fluoride contaminated working solution presented three samples under the study. The 50 mL of each fluoride contaminated working solution was used in respective plastic containers containing varied masses. The DW with varied pH served as a control. The Fe^0 materials in plastic containers were evenly submerged in measured 50 mL DW and working solutions. All systems received respective experimental treatment conditions (i.e., disturbed and non-disturbed); disturbed treatment was used to represent intermittent system swirling for 1 minute at 12 hours interval. All systems were allowed to run in triplicate and used average results only. An identical setup was concurrently reproduced but with the Fe^0 component coated by Red oxide primer. The summary of the experimental setup is available in Table 1. The experiment extended for two days at room temperature (23±2 °C).

Table 2: Setup on an investigation of water defluoridation considering the co-solute effect, varied Fe^0 mass, treatment (disturbed and non-disturbed), and different initial pH values

S/N	Working Solution	Experimental Condition											
		0.1 g of SW						1.0 g of SW					
		Disturbed			Non-disturbed			Disturbed			Non-disturbed		
		pH 4.5	pH 7.0	pH 9.5	pH 4.5	pH 7.0	pH 9.5	pH 4.5	pH 7.0	pH 9.5	pH 4.5	pH 7.0	pH 9.5
1	DW												
2	DW + F												
3	DW + F + Cl												
4	DW + F + SO_4												
5	DW + F + NO_3												
6	DW + F + HCO_3												
7	DW + F + PO_4												

(ii) Fluoride and pH Measurements

Samples were collected by vacuum filtration through a 47-mm diameter, 0.45-µm pore size GN-Metricel membrane filters prior to fluoride analysis. Fluoride ion-selective electrode affixed on S975 Seven Excellence pH Meter (as an ion meter) using the mV mode enabled assessment of aqueous fluoride content. A calibration curve was initially prepared by recording the potential values for a range of fluoride solutions of seven different concentrations (i.e., 0.00, 1.00, 10.00, 20.00, 30.00, 40.00 and 50.00 mg/L). The TISAB (pH 5.4±0.1) solution in a 1:1 was used to adjust standards and samples to the same ionic strength and pH; the final fluoride concentrations were calculated from the calibrations curve using measured potential values. Final pH values were measured prior to sample filtration through an S975 Seven Excellence pH Meter.

(iii) Iron Measurements

The difference between: (a) Unused identical SW masses and (b) Non-corroded SW after washing out the corroded and rusted part with DW enabled the computation of the iron used for corrosion and rust processes. Each category of these SW materials was prepared according to Sakai (2015) protocol and analyzed by an Inductively Coupled Plasma (ICP) instrument.

3.2.4 Expression of Experimental Results

(i) Actual Fluoride Concentrations (C) Correction after two Days (Equation 16)

$$C = \frac{[C_f \times V_f]}{[V_e + V_f]} \qquad (16)$$

Where C_f is the final/measured fluoride concentration; V_f is the final sample volume (after sample filtration); V_e evaporated sample volume (from respective samples with Fe^0 coated by Red oxide primer).

(ii) Fluoride Removal Efficiency (E) was Computed Using Equation (17) below from actual Fluoride Concentration (C)

$$E = \left[1 - \left(\frac{C}{C_o}\right)\right] \times 100 \qquad (17)$$

Where C_0 is the initial fluoride concentration of the prepared working solution.

(iii) Amount (%) of Iron Corrosion Products (Corroded + Rusted)

$$FeCPs = \left(\frac{m_o - m}{m_o} \right) x\,100 \qquad (18)$$

The experimental SW mass (0.1g or 1.0g) m, is a respective non-corroded SW mass after washing out the corroded and rusted part with DW.

3.2.5 Characterization

This section involved the characterization of corroded steel wool before: (a) In distilled and after (b) In 20 mg/L Fluoride solution. All characterization instruments were available at the Innovative Design and Integrated Manufacturing Laboratory, School of Mechanical and Aerospace Engineering, Seoul National University - Korea. Energy Dispersive X-Ray Spectroscopy (EDS) attached to the FESEM was used to elucidate different typical phases formed after reactions with fluoride and co-solutes and the monometallic nature of the steel wool. The X-Ray Photoelectron Spectroscopy (XPS) was used to address the actual bonding of the fluoride ions to iron.

CHAPTER FOUR

RESULTS AND DISCUSSION

4.1 Results

4.1.1 Characterization of Steel Wools

(i) Elemental Composition of Steel Wool

Tested steel wools were characterized in terms of elemental composition to identify any contaminant that will alter the defluoridation experiment by enhancing or retarding anticipated removal efficiencies. Elemental composition characterization is presented in Table 3.

Table 3: Major characteristics of tested Fe^0 SW specimens

Material Code	Diameter (mm)	Grade number	Name	Elemental composition (%)					
				Fe	Co	Cu	Pb	Ni	Cr
SW1	0.025	0000	Super Fine	99.15	0.01	0.03	0.40	0.09	0.32
SW2	0.035	000	Extra Fine	99.21	0.05	0.12	n.d.	0.16	0.47
SW3	0.04	00	Very Fine	99.25	0.05	0.16	n.d.	0.11	0.43
SW4	0.05	0	Fine	99.08	0.05	0.27	n.d.	0.11	0.49
SW5	0.06	1	Medium	98.37	0.05	1.00	n.d.	0.11	0.45
SW6	0.075	2	Medium Coarse	99.14	0.04	0.27	n.d.	0.10	0.45
SW7	0.09	3	Coarse	98.69	0.05	0.40	0.40	0.14	0.33
SW8	0.1	4	Extra Coarse	99.27	0.04	0.28	n.d.	0.10	0.30
SW9	0.04	00	Very Fine	99.62	0.01	0.02	n.d.	0.03	0.32

Origin: China (SW1 to SW8); Tanzania (SW9); Brand New (SW1 to SW8); Red Devil (SW1 to SW8); Lana de Acero (SW1 to SW8); Super Shine (SW9). The elemental composition (%) was determined in this study. Al, As, and Zn were not detected (n.d.).

Metal composition in tested steel wool materials followed the order of Iron >>> Chromium > Copper > Nickel > Cobalt > Lead. Iron contents were more than 98% compared to other tested metal components.

(ii) Suitability of the Approach

Figures 2 and 3 compare the results of SW 9 dissolution in three different solutions, i.e. 2 mM EDTA, 2 mM Phen, and 6 mM Phen. The EDTA dissolves far more iron than Phen (up to 90 mg L^{-1} vs Less than 40 mg L^{-1}). Inversion during sampling sessions slightly enhanced iron dissolutions in both solutions. There is no significant difference in the extent of iron dissolution in 2 mM and 6 mM Phen; furthermore, 6 mM Phen (Fe:Phen = 1:3) corresponds to 2 mM EDTA (Fe:EDTA = 1:1) in the stoichiometry of Fe complexation by both agents. Explanations of observed variations behaviours from such figures tend to consider the system's chemistry, i.e Fe^0 is corroded by water (H_2O or H^+) according to Equation 19.

$$Fe^0 + 2\ H^+ \Longrightarrow Fe^{2+} + H_2 \quad (19)$$

$$Fe^{2+} + Phen \Longrightarrow (Fe\text{-}Phen)^{2+} \quad (20)$$

$$4Fe^{2+} + O_2 + 2\ H^+ \Longrightarrow 4Fe^{3+} + 2\ OH^- \quad (21)$$

$$Fe^{3+} + EDTA \Longrightarrow (Fe\text{-}EDTA)^{3+} \quad (22)$$

$$FeOOH + EDTA + 3\ H^+ \Longrightarrow (Fe\text{-}EDTA)^{3+} + 2\ H_2O \quad (23)$$

Under Phen chelate, Fe^{2+} is complexed to form a very stable Fe-Phen complex (Equation 20), which blocks the Fe^{2+} oxidation by dissolved oxygen (Equation 21). In the presence of EDTA, Fe^{2+} oxidation to Fe^{3+} (Equation 21) is rather accelerated because $(Fe\text{-}EDTA)^{3+}$ is more stable than $(Fe\text{-}EDTA)^{2+}$. The resulting Fe^{3+} is then complexed by EDTA (Equation 22). It should be recalled that $(Fe\text{-}EDTA)^{3+}$ is not destabilized by many inorganic reducing agents, including hydroxylamine. Hydroxylamine is used in the standard spectrophotometric method to reduce Fe(III)-species prior to the formation of the characteristic orange complex of Fe(II)-Phen (Elmagirbi *et al.*, 2012). Lastly, amorphous Fe(III) corrosion products are (at least partly) dissolved in EDTA (Equation 23). Note that amorphous Fe(II) corrosion products would be dissolved both in EDTA and Phen.

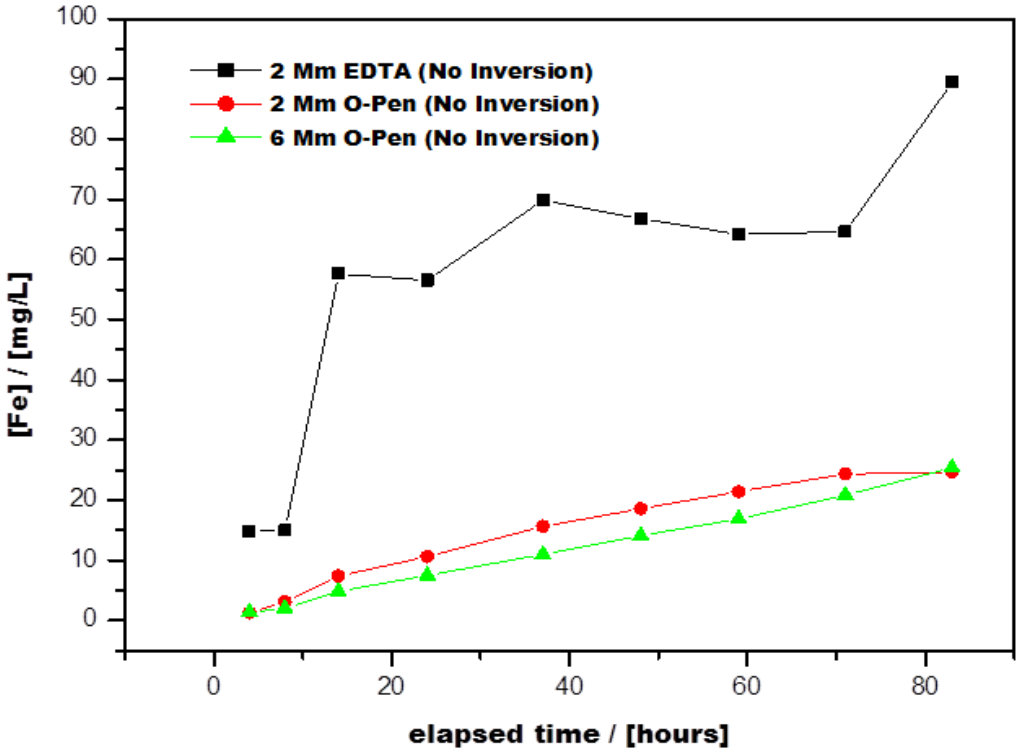

Figure 2: Comparison of Iron dissolution in 2 mM EDTA and 2 mM Phen (No Inversion)

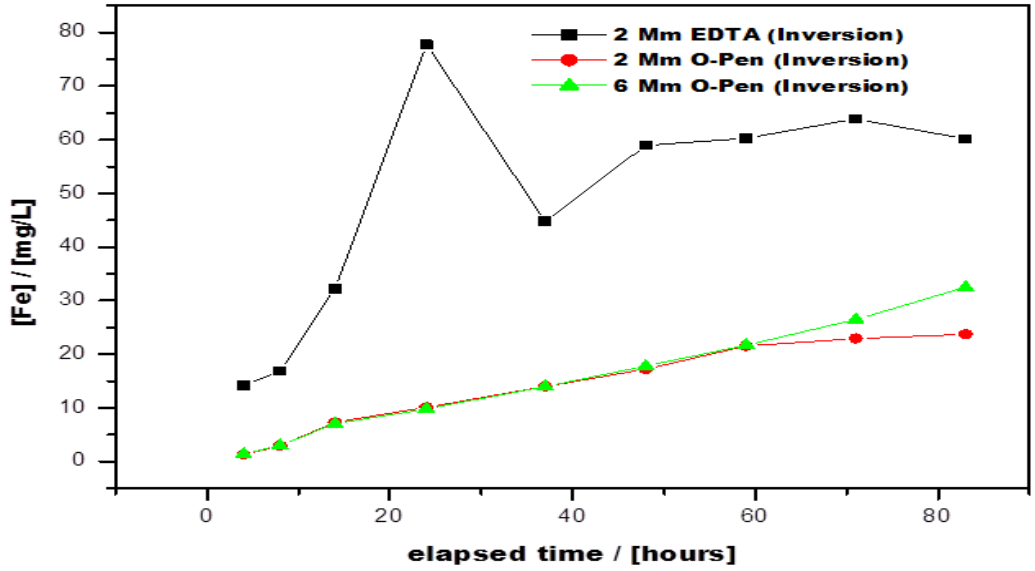

Figure 3: Comparison of Iron dissolution in 2 mM EDTA and 2 mM Phen (Inversion conditions)

(iii) Characterization of Steel Wool in Ethylene Diamine Tetra Acetic Acid and 1,10 Phenanthroline

After the approach have been confirmed to be suitabile, testing on eight sample steel wool for characterization purpose was subjected in respective 2 mM EDTA and 2 mM Phen (Fig. 4 and 5).

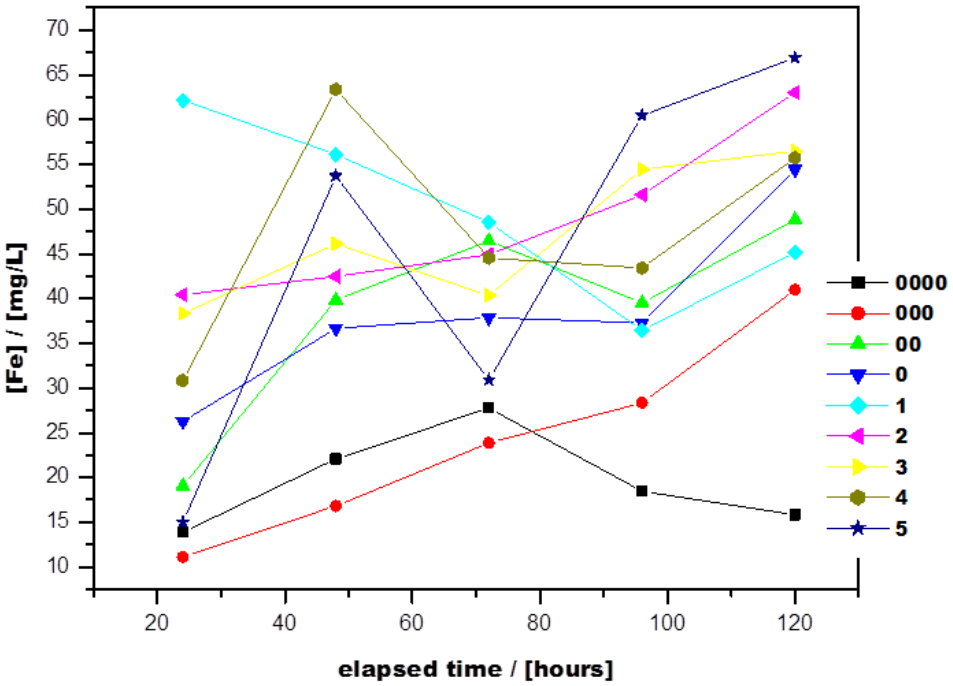

Figure 4: Characterization of SW in 2 mM EDTA solution for 120 monitored hours

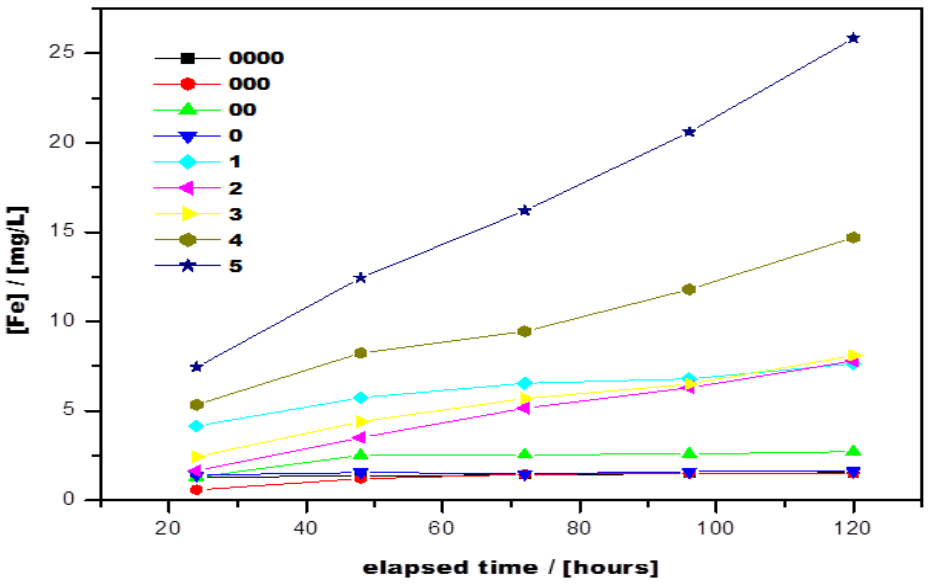

Figure 5: Characterization of SW in 2 mM Phen solution for 120 monitored hours

Figures 2 and 3 show no influence in the Phen method by dissolved oxygen or atmospheric corrosion products on Fe^0 as contrasted by the EDTA method. Thus the Phen method is free from an inherent limitation of the EDTA method making its application for characterizing fine Fe^0 specimens containing large amounts of atmospheric corrosion products challenging (Btatkeu-K *et al.*, 2013; Hildebrant, 2018). Hildebrant (2018) recently presented an original approach to address this challenge. This consisted of reducing the mass of Fe^0 SW from 0.1 g to 0.01 g in 50 mL of the EDTA solution. Even then, a linear relationship between the elapsed time and the dissolved iron concentration was difficult to obtain (Hildebrant, 2018). The perfect linearity observed in Fig. 2, 3, 4, and 5 for Phen confirms that using the Phen method, practically only Fe^0 oxidative dissolution is characterized.

Table 4: Corresponding correlation parameters (k_{EDTA}, k_{Phen}, b, R^2) for the tested Fe^0 SW

Sample	EDTA				O-Phen			
	k_{EDTA} (mg h^{-1})	b (mg)	N (-)	R^2 (-)	k_{Phen} (mg h^{-1})	b (mg)	N (-)	R^2 (-)
SW1	2.320	0.600	5	0.9256	0.072	0.055	5	0.9931
SW2	0.525	2.400	5	0.5338	0.1960	0.3050	5	0.9957
SW3	4.505	(-)1.025	5	0.997	0.2830	(-) 0.03	5	0.9974
SW4	1.385	0.250	5	0.7809	0.4670	(-) 0.215	5	0.9956
SW5	4.620	0.525	5	0.988	0.5430	(-) 0.065	5	0.9635
SW6	3.765	(-)2.775	5	0.9342	0.1090	(-) 0.055	5	0.9539
SW7	3.090	0.300	5	0.8992	0.3840	(-) 0.245	5	0.9700
SW8	4.225	(-)2.275	5	0.9216	0.8840	(-) 0.615	5	0.9808
SW9	4.805	(-)2.45	5	0.7985	1.2980	1.1000	5	0.9984

As a rule, the more reactive a material is under a given conditions the larger the k value is. Experimental conditions: [EDTA] = [Phen] = 2 mM, room temperature 23 ± 2 °C, [Fe^0] = 0.10 g, and Vsolution = 50 mL. The k_{EDTA}, k_{Phen} and b-values were calculated using Origin 6.0. The k values from Table 2 enable better classification of the order of reactivity of the tested SW:

In EDTA: SW2 < SW4 < SW1 < SW7 < SW6 < SW8 < SW3 < SW5 < SW9.

In Phen: SW1 < SW6 < SW2 < SW3 < SW7 < SW4 < SW5 < SW8 < SW9.

4.1.2 Defluoridation by Metallic Iron

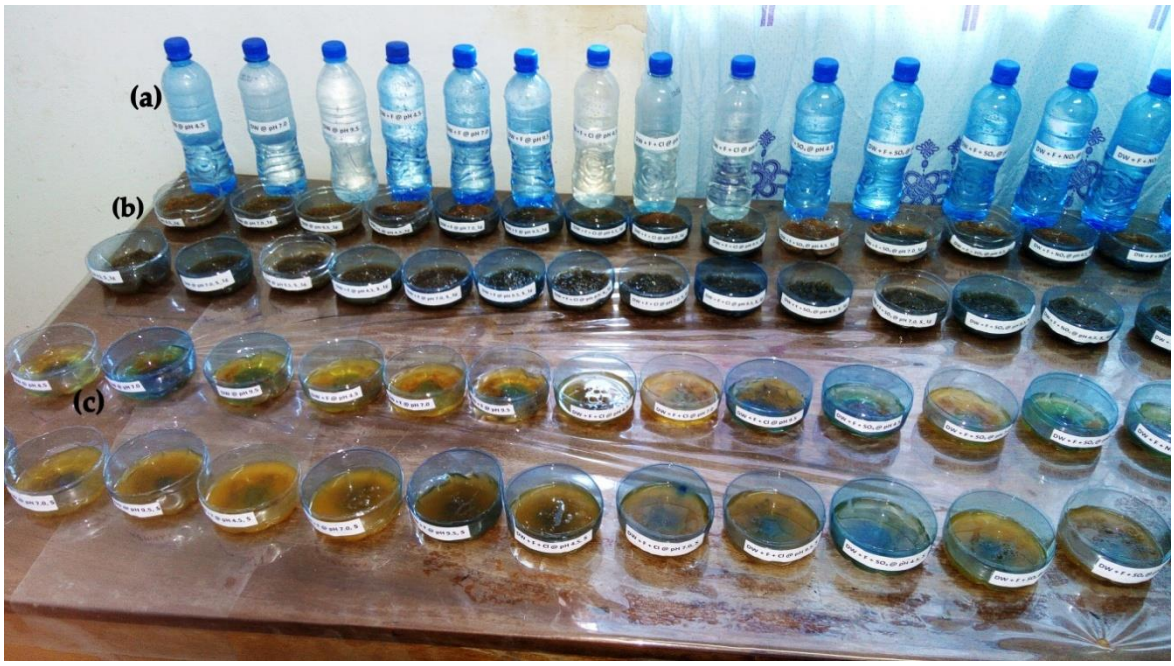

Plate 1: An optical picture of the actual laboratory set-up showing, from left to right, the (a) prepared samples (b) corroded 1.0 g of SW in non-disturbed (first row) and disturbed (second row), and (c) corroded 0.1 g of SW in non-disturbed (first row) and disturbed (second row)

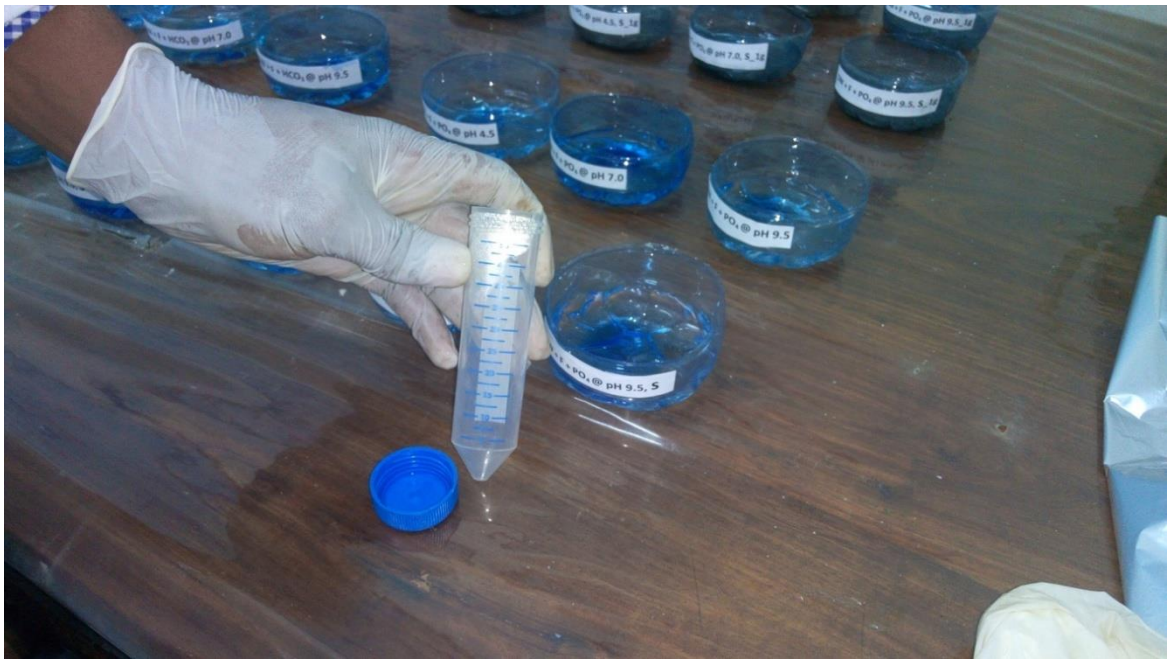

Plate 2: Conventional laboratory assay tube (handheld in the picture) and plastic experimental designed containers (on the bench in the picture)

Most preliminary fluoride results were observed to be higher than those in the used working solutions. The experiment was reset with a separate concurrent setup, where Fe^0 was coated by

red oxide primer to inhibit corrosion; this enabled simulation of individual sample evaporation rates for computing actual fluoride concentration after two days. Dilute acetic acid and ammonia solutions were used to adjust experimental pH values (that reflects current water quality guidelines and natural water properties) due to their negligible influences on corrosion rates (Fajardo *et al.,* 2008) as contrasted by Velazquez-Jimenez *et al.* (2015) on acetic acid with enhanced defluoridation rates. The use of weak acid enabled avoiding the introduction of undesirable co-solutes content available from conventional acids, e.g. HCl, H_2SO_4, H_3PO_4, and HNO_3 that otherwise would have modified desirable co-solute sat values. Fluoride contaminant of 23±2.0 mg/L was used based on groundwater average global scenario values (Parashar *et al.*, 2019), where co-solutes were also assigned the same strength for simulating equimolar ligand influences (Heimann *et al.,* 2018b).

(i) The 0.1 g of Steel Wool, Systems

In all studies under this category, FeCPs had flaky and brittle properties. At least 99% of these FeCPs were observed to have a brick-red colour. The 79±13% of the original iron was not corroded.

Disturbed

Higher FeCPs were observed under disturbed conditions. The E values can be summarized in Fig. 2 based on initial pH values and respective working solution systems:

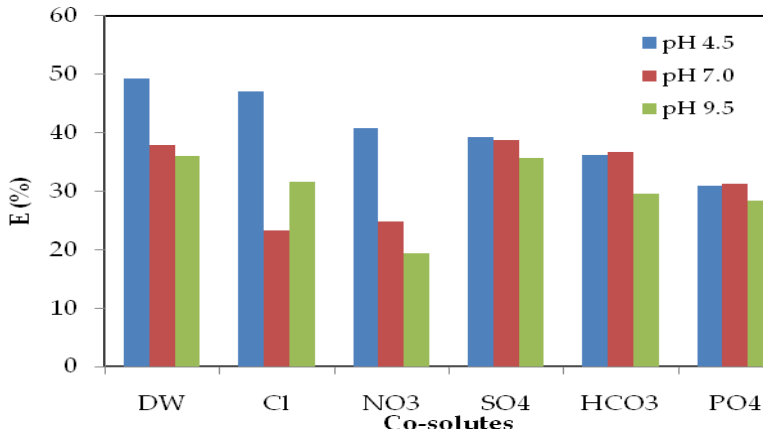

Figure 6: Effect of different (i) Co-solutes and (ii) initial pH values in defluoridation efficiency by 0.1 g Fe^0 under disturbed experimental conditions

The phosphate system had final pH values between 6.36 and 6.54; other systems had their final pH values in a range of 5.64 to 6.37. To all examined systems, E values were generally highest at initial pH 4.5 and lowest at Initial pH 9.5. Reference systems had comparable E values at initial pH values of 7.0 and 9.5. The HCO_3 and PO_4 systems had respective comparable E values at pH 4.5 and 7.0. The SO_4 system had comparable E values at all initial pH values.

Non-disturbed

Relative less FeCPs were observed under non-disturbed conditions. The E values can be summarized in Fig. 7 based on initial pH values and respective working solution systems:

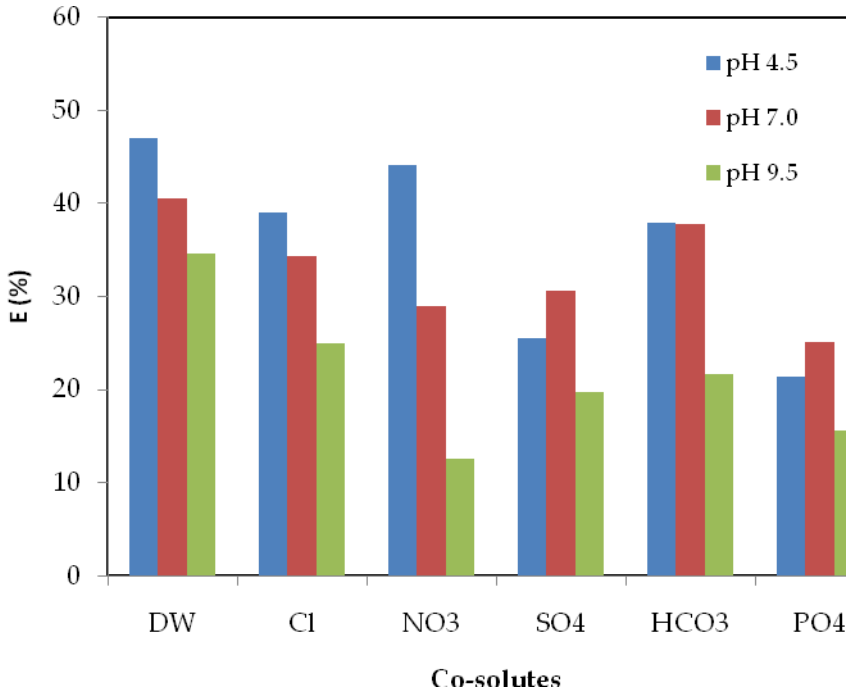

Figure 7: Effect of different (i) Co-solutes and (ii) initial pH values in defluoridation efficiency by 0.1 g Fe^0 under non-disturbed experimental conditions

The phosphate system had final pH values between 6.32 and 6.59; other systems had their final pH values in a range of 5.69 to 6.25. To all examined systems, E values were generally highest at initial pH 4.5 and lowest at initial pH 9.5. The HCO_3 system had comparable E values at pH 4.5 and 7.0. The SO_4 system had the highest E value at initial pH of 7.0.

(ii) The 1.0 g of SW, Systems

The FeCPs were characterized by poor flaky and brittle properties in all studies under this category, mostly being finely suspended. The FeCPs were observed to have variable colours. The 90±2% of the original iron mass was found un-corroded.

Disturbed

More than 99% of FeCPs formed in all systems, except PO_4, were black. Traces of greenish rust were also noted to exist. All PO_4 systems were characterized by more than 90% green FeCPs, where traces of black FeCPs were also observed. The E values can be summarized in Fig. 4 based on initial pH values and respective working solution systems:

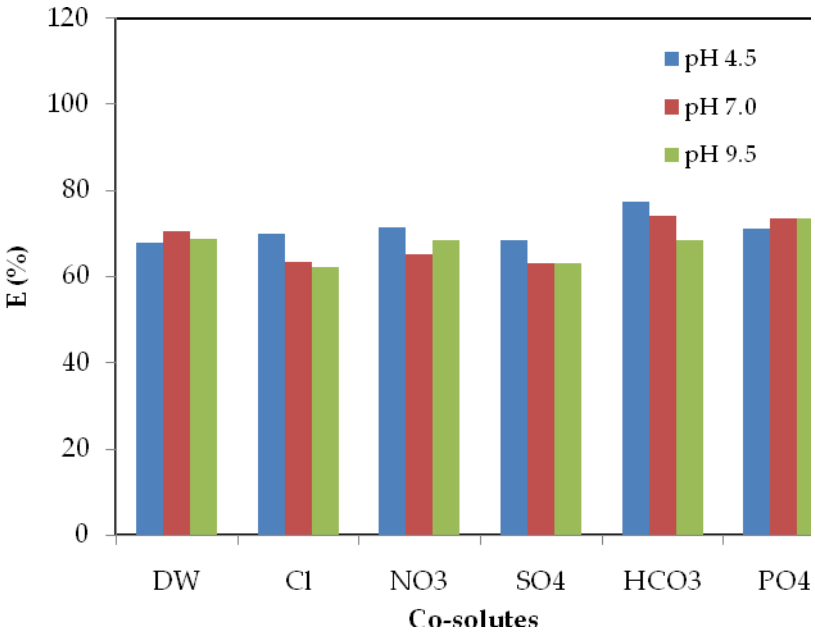

Figure 8: Effect of different (i) Co-solutes and (ii) initial pH values in defluoridation efficiency by 1.0 g Fe^0 under disturbing experimental conditions

The phosphate system with an initial pH value of 9.5 had a final pH value of 5.72 and presented a high E value system at this initial pH. Other systems had their final pH values in a range of 6.24 to 7.18. To all examined systems, E values were generally highest at initial pH 4.5 and lowest at initial pH 9.5. All systems had respective comparable E values at all initial pH values.

Non-disturbed

More than 90% of FeCPs formed in all systems, except PO_4, were black. Traces of greenish rust were also noted to exist. All PO_4 systems were characterized by more than 80% green FeCPs, with traces of black FeCPs. In all systems, the top layer was fairly brick-red coloured. The E values can be summarized in Fig. 5 based on initial pH values and respective working solution systems:

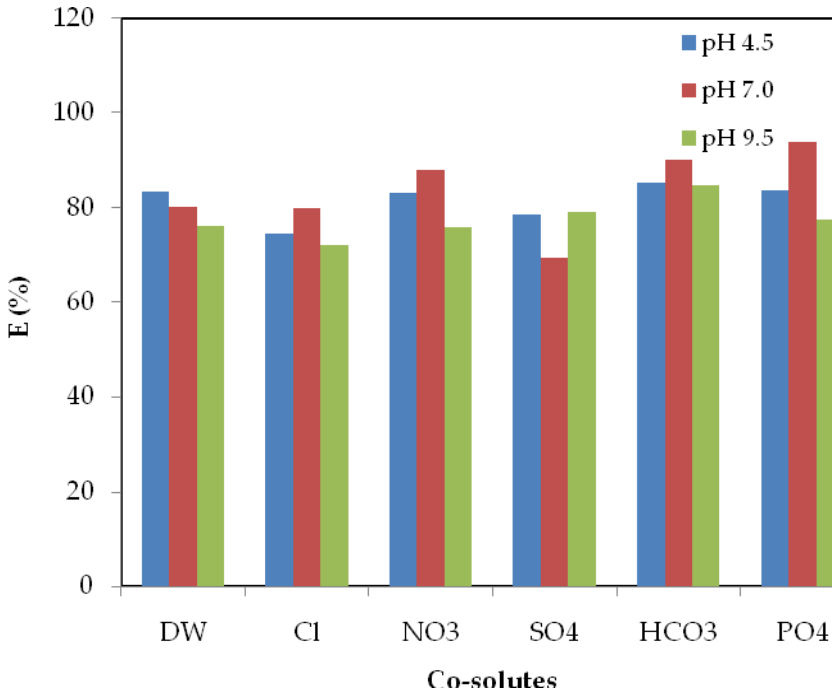

Figure 9: Effect of different (i) Co-solutes and (ii) initial pH values in defluoridation efficiency by 1.0 g Fe^0 under non-disturbed experimental conditions

Bicarbonate system with an initial pH value of 9.5 had a final pH value of 4.62 and presented a high E value system at this initial pH. Other systems had their final pH values in a range of 5.63 to 6.26. To all examined systems, E values were generally highest at initial pH 7.0 and lowest at initial pH 9.5. All systems had fair respective comparable E values at all Initial pH values.

(iii) Material Characterization

Material characterization was done in two stages: Initially, the steel wool was characterized before adoption with fluoride ions and co-solutes, and finally, the steel wool was characterized after being reacted with both fluoride ions and co-solutes. The whole characterization process was done as follow:

Energy Dispersive X-Ray Spectroscopy Analysis

At first the Energy Dispersive X-Ray Spectroscopy was used to characterize the steel wool as shown in Fig. 10. Figure 10 (a) shows the corroded and rusted SW variation in: (a) Distilled water, and 10(b) 20 mg/L fluoride solution. Fluoride peak in 10(b) confirms the occurrence of fluorine reaction with iron materials in the system.

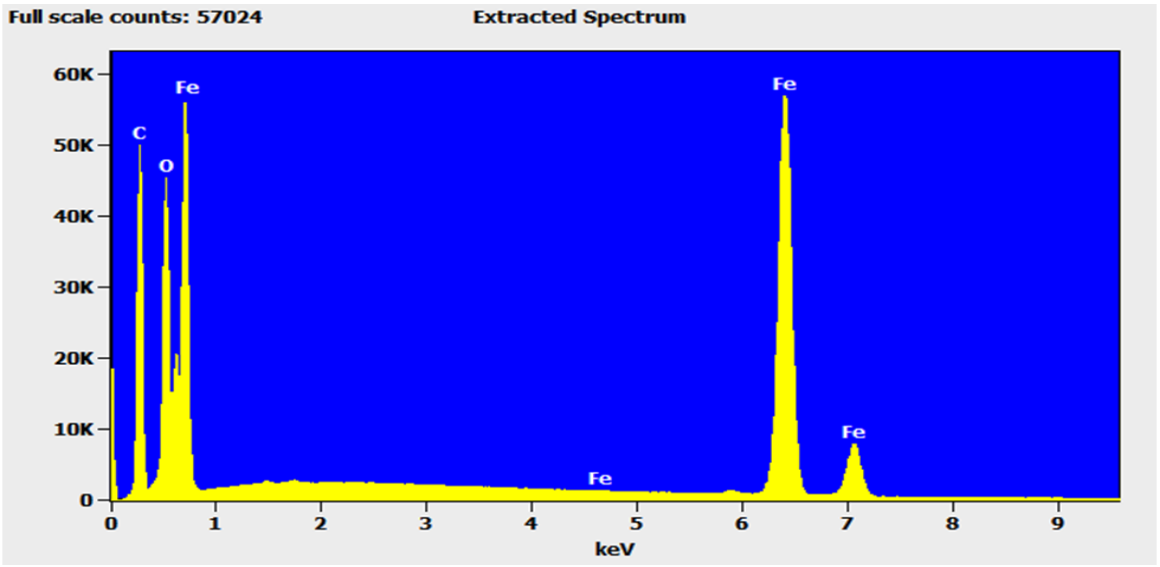

(a)

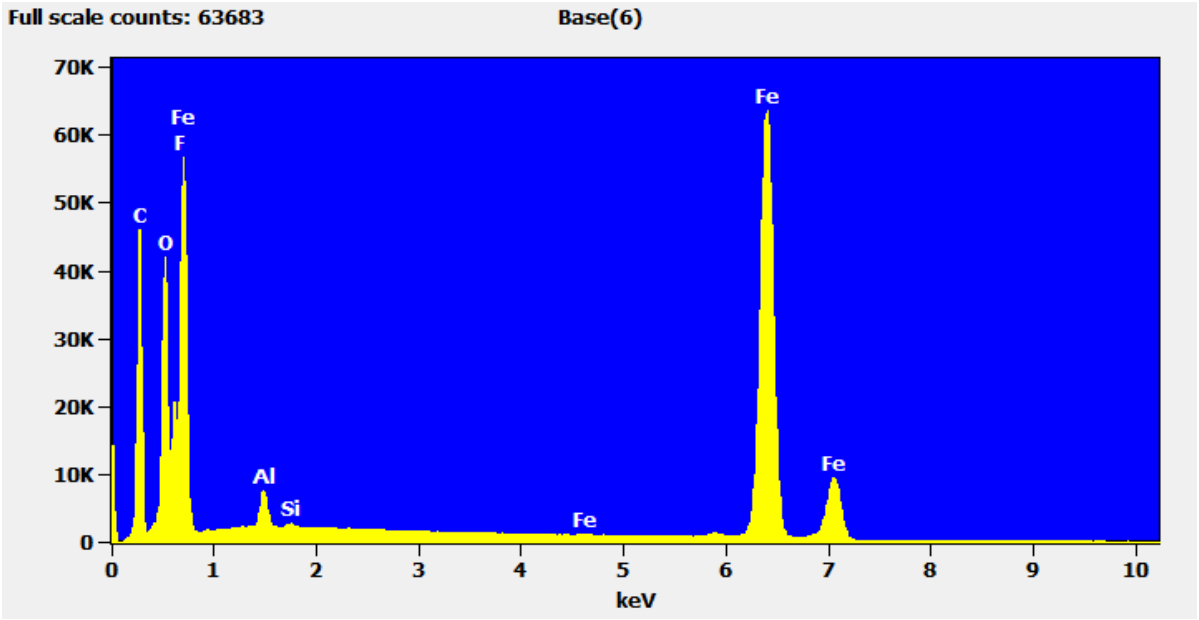

(b)

Figure 10: Energy Dispersive X-Ray Spectroscopy spectrum of corroded steel wool at initial pH 4.5 in (a) distilled water, (b) 20 mg/L fluoride solution

X-Ray Photoelectron Spectroscopy Analysis

X-Ray Photoelectron Spectroscopy was also used to characterize the steel wool as shown in Fig. 11. Figure 11 (a) and (b) show that fluoride reaction with iron materials occurred due to the presence of fluorine element with F 1s peak at 685 eV. Figure 11(b) shows that Fe 2p have slightly higher binding energy compared to the same characteristic Fe 2p in Fig. 11 (a).

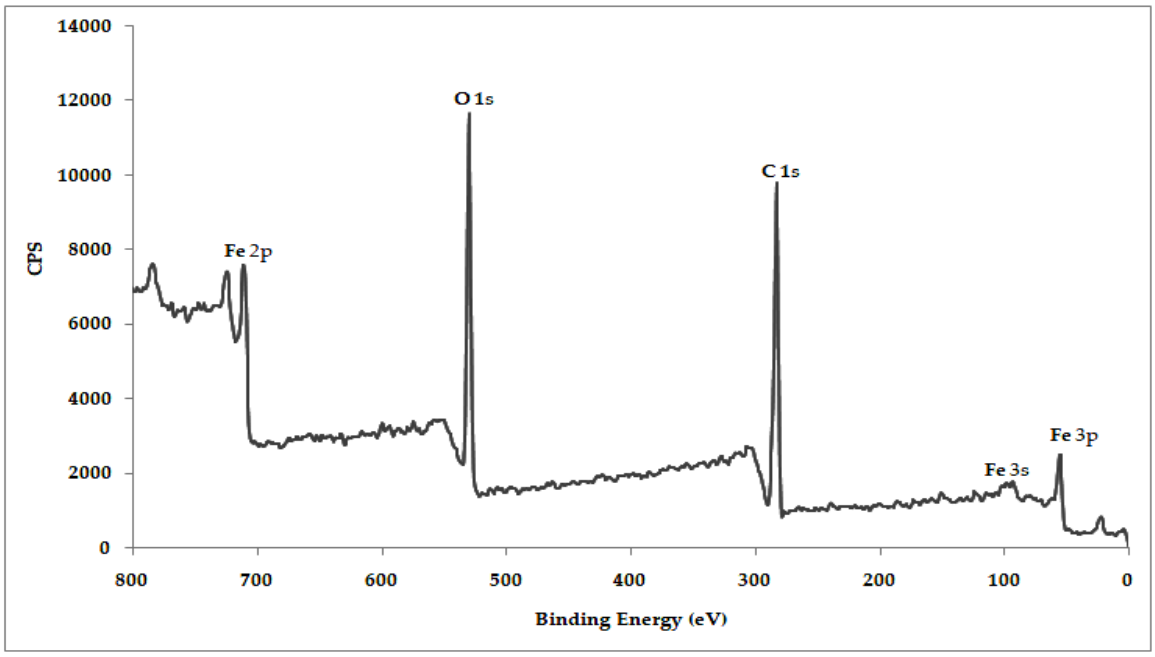

(a)

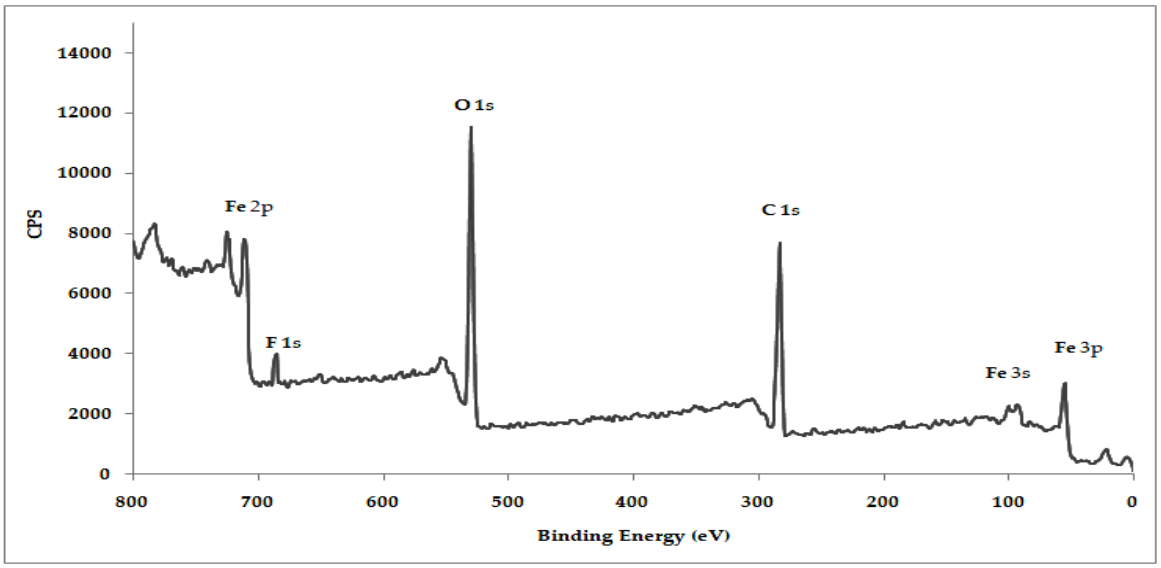

(b)

Figure 11: X-Ray Photoelectron Spectroscopy Spectra of corroded steel wool at initial pH 4.5 in (a) distilled water, (b) 20 mg/L fluoride solution

Field Emission Scanning Electronic Microscopy Analysis

Finally, Surface morphology of corroded and rusted SW *was* also characterize by using Field Emission Scanning Electronic Microscopy in both: (a) Distilled water, and (B) 20 mg/L solution. Micrographs in Fig. 12 (a) show mainly iron hydroxide nanoparticles and trace oxides of other contaminants in SW used material. The FESEM image in Fig. 12 (b) shows intensive spores like structure due to fluoride and other elements in iron hydroxides formed.

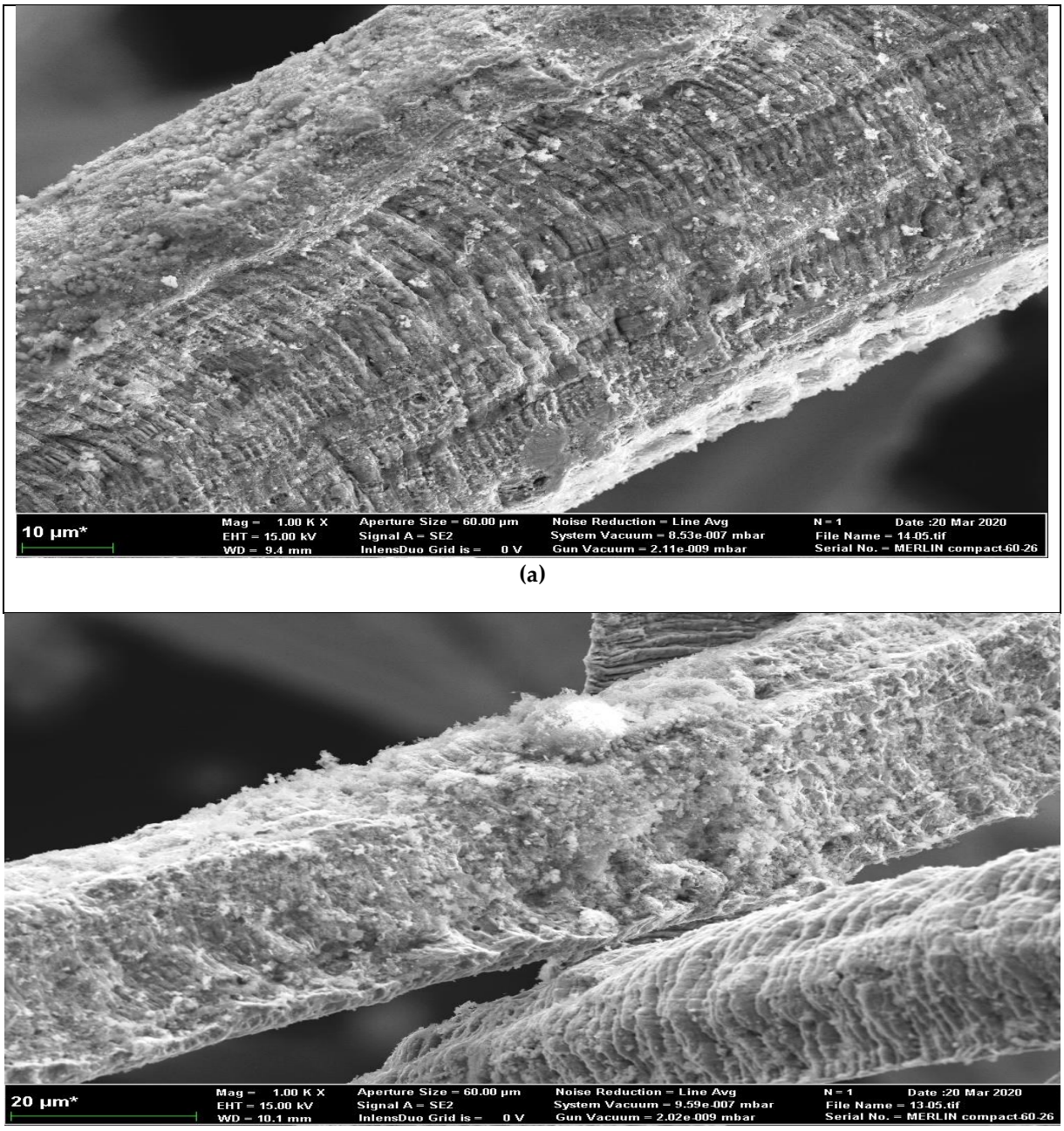

(a)

(b)

Figure 12: Field Emission Scanning Electronic Microscopy micrographs of corroded steel wool at initial pH 4.5 in (a) distilled water, (b) 20 mg/L fluoride solution

4.2 Discussion

The availability of water and oxygen on iron materials determines the nature and extent of FeCPs formation. Major variations were observed in this study following the modification of conventional laboratory assay tubes, which are usually of more extended depth with a small top diameter (Plate 2). Plastic containers used were aimed at facilitating more oxygen which is a complementary corrosion agent. Systems with 0.1 g of SW formed brick-red FeCPs, characteristic of high oxygen concentrations that preferentially support iron (III) reaction products. Systems with 1.0 g of SW had more black FeCPs depicting low oxygen concentration, which indicates that iron (II) reaction products are favoured, e.g. wüstite, lodestone or magnetite (Fe_3O_4). Generally, there are 16 available oxides of iron in which only three are solely based on iron (II), whereas others are more in the iron (III) state (Cornell & Schwertmann, 2003). This section emphasizes much on defluoridation feasibility in conventional Fe/H_2O Systems under consideration of associated influences from various: (a) Co-solute types, (b) initial pH values, and (c) treatments employed.

4.2.1 Characterization of SW material before and after adsorption/reaction with Fluoride ions and co-solutes

(i) Spectra

Figure 10 shows the corroded and rusted SW variation in distilled water: (a) and 20 mg/L fluoride solution (b). Fluoride peak in (b) confirms the occurrence of fluorine reaction with iron materials in the system.

(ii) X-Ray Photoelectron Spectroscopy Spectra

The XPS spectra in Fig. 11 (a) and (b) show that fluoride reaction with iron materials occurred due to the presence of fluorine element with F 1s peak at 685 eV in Fig. 11 (b). Figure 11(b) shows that Fe 2p have slightly higher binding energy compared to the same characteristic Fe 2p in Fig. 11 (a). Such variations are confirmed by Jones *et al.* (2018), which depicts changes in bonding, mainly from the strong electronegative fluorine element, i.e. the more ionic iron ligand bond becomes, the higher the binding energy (Grosvenor *et al.,* 2004). This observation further confirms the fluoride reaction with iron in analyzed corrosion products.

(iii) Field Emission Scanning Electronic Microscopy Micrographs

Surface morphology of corroded and rusted SW in: (a) distilled water and (b) 20 mg/L solution showed significant variations. Micrographs in Fig. 12 (a) show mainly iron hydroxide nanoparticles and trace oxides of other contaminants in SW used material. The FESEM image in Fig. 12 (b) shows intensive spores like structure due to fluoride and other elements in iron hydroxides formed. Fluoride has proven to accelerate corrosion and rusting of iron (Ghosh *et al.,* 2003) due to excessive FeCPs formed in Fig. 12 (b) as contrasted from Fig. 12 (a), hence its aqueous reaction with iron materials and its removal.

4.2.2 Fluoride Decontamination Processes in Conventional Fe/H_2O System

The FeCPs exhibit aqueous fluoride remediation due to: (a) Fluoride ion size being as small as that of hydroxyl ion, (b) Fluoride nucleophilic character is strong, and (c) The FeF bond is strong (Cornell & Schwertmann, 2003; Zhang *et al.,* 2017; Dhillon & Kumar, 2019). The surface area and porosity of FeCPs determine the interaction efficiency with aqueous contaminants; this is why adsorption is a major technical category for nano-scale iron-based defluoridation studies where water becomes free from pollutants and suitable for domestic uses (Zhang *et al.,* 2017). For conventional Fe/H_2O System, Ndé-Tchoupé *et al.* (2019a) delineated that co-precipitation with nascent FeCPs is a primary defluoridation mechanism over adsorption by aged FeCPs. These observations align with 1.0 g based systems where iron (II) products, e.g. Magnetite, which is non-porous (Cornell & Schwertmann, 2003) are favoured. Thus fluoride removal efficiencies become less appreciable by adsorption as abundant aqueous fluoride ions fail to penetrate within the formed impervious FeCPs, leaving nascent FeCPs responsible for mostly observed removals. The 1.0 g systems become obliged to treat multi-contaminants due to the realization of both ion-selective and non-ion selective (co-precipitation and size exclusion) mechanisms (Naseri *et al.,* 2017) making it less frugal. However, significant removal of fluoride was observed in 0.1 g systems where iron (III) based FeCPs are preferred. This was attributed to the nature of such FeCPs with substantial porosity to facilitate significant fluoride adsorption over co-precipitation. Furthermore, Hiemstra and Van Riemsdijk (2000) showed that fluoride adsorption was twice as high in low surface area compared to the high surface area of the same FeCPs (i.e., Goethite); the reason behind this suggested that in small surface area, goethite could have more serious imperfections than in the high surface area. In this case, controlling FeCPs formation strictly defines the defluoridation feasibility in conventional

Fe/H_2O systems. Low defluoridation efficiencies in conventional Fe/H_2O Systems (Heimann *et al.,* 2018a, 2018b; Ndé-Tchoupé *et al.,* 2019a) that usually presents limited adsorption sites are further justified based on versatile FeCPs active functional groups that also adsorb cations (Cornell & Schwertmann, 2003; Gogoi *et al.,* 2018) available as counter-ion from used preparation compounds, and contaminants in parent used Fe^0 materials. With such low defluoridation efficiencies, Heimann (2018) conducted defluoridation using two identical columns in series but could not improve fluoride removal efficiency. The abnormality can be explained herein that a high concentration of fluoride (together with co-solutes) in water presents high ionic strength. This promotes fluoride removal by surface precipitation with iron as FeF_3 (Cornell & Schwertmann, 2003; Sarkar *et al.,* 2006). But at relative low aqueous ionic strength, defluoridation processes explained above prevails, and subsequent column becomes inadequate for considerably improved removal efficiency.

(i) Effect of Co-solutes

Natural water contains other anions in addition to elevated fluoride contaminants, their competitive effects in water defluoridation using FeCPs have been widely studied (Table 5), the emphasis is given to studies realizing defluoridation experiments in the presence of co-solutes.

Table 5: Effect of co-solutes in defluoridation studies with consideration of Initial fluoride concentration, $[F]_o$; Weight of iron materials used, Fe^0; Water sample volume, V; Treatment condition and Operation mode, TO; Contact time, t; Initial pH values, pH_0; final pH values, pH_f; and maximum fluoride removal efficiency, E

$[F]_o$ (mg/L)	Fe_o (g)	V (mL)	TO	t (h)	pH		Co-solutes Effects		E (%)	Reference
					pH_o	pH	Large	Low*		
2.45	0.1	10	Shaken at 45 rpm in batch systems	24	7.4	7.4±2	HCO_3 > Cl	SO_4, PO_4, NO_3	~45	Martínez-Miranda *et al.* (2011)
114	1	1000	Jar test Batch systems	48	4	-	PO_4 > SO_4	Cl, NO_3	18	Huang *et al.* (2011)**
25	0.05	20	Shaken at 60 rpm in batch systems	8	-	-	HCO_3	SO_4, PO_4, Cl SiO_3, NO_3,	50	Iiu *et al.* (2016)
4	0.05	50	Batch systems	0.03	7 - 8	-	CO_3 & PO_4 above 10 times higher than [F]	SO_4, Cl, NO_3 even at 25 times higher than [F]	100	Zhang *et al.* (2017)
22.5	100	-	Column systems	7200	6.9±0.2	7.8±0.5	Cl >>>HCO_3	-	40	Heimann *et al.* (2018b)
9.43	0.25	25	Batch systems	0.75	6.1	7.8*	CO_3 > SO_4 > HCO_3	Cl, Br, NO_3	89	Gogoi *et al.* (2018)
20	0.1	22	Batch systems	1800	5 & 8	7.8	-	-	30	Ndé-Tchoupé *et al.* (2019a)

* Co-solutes with no or non-considerable defluoridation effect of ±10% from the reference
** Fe^0 weight and volume were deduced from 1 g/L of FeCPs used in all experiments
* **Based on calculated Isoelectric point values

Table 5 depicts a significant variation on the type of interfering and less or non-interfering co-solutes from different studies; however, excellent defluoridation efficiencies are reported in control systems, i.e. with only fluoride contaminant in test water. In either nano-scale iron or conventional Fe/H_2O System, HCO_3 consistently interferes with fluoride removal efficiencies due to the formation of inner-sphere surface complex, a property common in fluoride dissolution from rocks into groundwater (Liu *et al.,* 2016). In this study, HCO_3 was only significant on observed lower E values in 0.1 g systems; but 1.0 g systems were not remarkably affected by such a strong co-solute. This can be attributed to the swift formation of high quantity FeCPs in 1.0 g systems compared to those of 0.1 g systems, where: (a) Rapid pH adjustments below isoelectric points were realized, giving satisfactory defluoridation conditions of final pH values between 5.63 and 7.18, and (b) Quantitative removal of all contaminants due to formation of more FeCPs.

Most reported higher E values in Table 5 were based on low: (a) V and (b) $[F]_0$ used in their experimental setup. Thus comparing such results with current conventional Fe/H_2O System performance that mostly utilizes higher V and $[F]_0$ can propagate a misleading conclusion (Ndé-Tchoupé *et al.,* 2019a) and prosper a complete abandonment of this research side. The 1.0 g systems had a maximum of 93.95% fluoride removal efficiency, whereas 0.1 g systems only presented a maximum of 47.06% from one of all explored study treatments; whereby, the amount of iron consumed to provide such results varied significantly. It was noted that 0.1 g systems used 26±7% of Fe^0 to achieve such E values as contrasted by 1.0 g systems that used almost 5 times Fe^0 for their observed E value; this is why Heimann *et al.* (2018b) commented on conventional Fe/H_2O System being in-demand of high iron materials and or thicker filters to accomplish desirable defluoridation efficiencies. In this case, 0.1 g systems showed significant achievement in defluoridation under the conventional Fe/H_2O System. In the present study, FeCPs were developed in solutions containing respective contaminants. Cornell and Schwertmann (2003) explored the influence of foreign compounds on the preferential formation of a particular iron oxide compound which behaves differently in remediation practices. Thus, observed E value qualities and variations are also attributed to this condition. In particular, PO_4 influenced E values in 0.1 g systems irrespective of initial pH values; significant inhibition on defluoridation were observed in un-disturbed treatments. The ability of PO_4 to dually coordinate two adjacent hydroxyl functional groups available on FeCPs may create surface precipitates that hinder further access to other ions; furthermore, suppression of the formation of porous

FeCPs in favour of non-porous FeCPs is evident in high PO_4 content systems (Cornell & Schwertmann, 2003). Contrasting from many observations in Table 5, NO_3 and Cl had profound defluoridation retardation effects on 0.1 g systems with initial pH values of 7.0 and 9.5.

Generally, the effect of co-solute in defluoridation can be observed to be significant in 0.1 g system. For 1.0 g systems, co-solute effects fall within ±10% variations from reference E values, hence considered to be insignificant in this study. Trend of co-solute influences in 0.1 g systems can be deduced as follows with ±10% rule for E value variations from respective references: (a) In disturbed treatment, at pH 4.5: $PO_4 > HCO_3 > SO_4$; at pH 7.0: $Cl > NO_3 > PO_4$; at pH 9.5: $NO_3 > PO_4 > HCO_3$ and, (b) In non-disturbed treatment, at pH 4.5: $PO_4 > SO_4 > HCO_3$; at pH 7.0: $PO_4 > NO_3 > SO_4$; at pH 9.5: $NO_3 > PO_4 > SO_4 > HCO_3 > Cl$.

(ii) Effect of pH

Many studies presented in Table 2 were also associated with defluoridation using Fe^0 considering initial pH variation effects on observed E values. Nano-scale iron-based defluoridation studies were found to possess a wide range of applicable pH values (i.e. 2 to 10) that enabled the achievement of desirable E values. However, E values associated with conventional Fe/H_2O systems were found to be affected by pH variations, and desirable E values were mostly achieved from pH 4 to 7. Such variations arise from associated decontamination modes, i.e. while nano-scale iron materials are subjected in studies, their high surface area and porosity enable fluoride decontaminations by complementary interactions of removal mechanisms. Thus, when one option is impaired due to pH influence, the other one works even though it could be less considerable, but the overall effect in such efficient materials becomes appreciable. In a conventional Fe/H_2O System, FeCPs are generated during experimentations. Thus, when Fe^0 materials are subjected to unfavourable initial pH conditions that diminish the occurrence of in-situ iron corrosion, defluoridation becomes impaired to low E values. In this study, significant variations were observed in 0.1 g systems where all working solution systems under respective initial pH values had higher E values in the order of pH 4.5 > pH 7.0 >>> pH 9.5; furthermore, the observed influence of co-solute on E values of these systems was the function of initial pH variation. For instance, the effect of HCO_3 on the reduction of E values was reduced at a low pH system which validates the suggestion of Millar *et al.* (2017) on reducing pH to low values for the same purpose. The NO_3 was observed to have a diminished effect of lowering E values of systems subjected at pH 4.5; these findings corroborate

observations on nitrate being rapidly transformed to ammonium (which equilibrates with the readily escaping ammonia gas) at lower pH values between 2 and 4.5 under Fe/H_2O systems (Vodyanitskii & Mineev, 2015). On the other hand, 1.0 g systems had overall comparable high E values satisfying the ±10% rule from the reference; thus, the quantitative formation of more FeCPs ruled out the influence of pH on observed E values. Most of the final pH values were below the WHO minimum drinking water guideline of 6.5, and this was attributed to hydrolysis processes that enabled dissolved iron to utilize hydroxides from the water molecule, leaving the proton in the solution that accounts for observed low pH values. This condition could also explain why PO_4 systems had relatively higher final pH values, as their high affinity on FeCPs functional groups significantly reduces the availability of aqueous iron that would otherwise exhibit substantial hydrolysis.

(iii) Effect of Experimental Disturbance

The aim of subjecting this study in this category was to assess any influence of disturbances associated with water movements across conventional Fe/H_2O filter-based systems. Unlike 1.0 g systems, disturbance in 0.1 g systems enhanced E values appreciably. Since 1.0 g systems exhibited quantitative defluoridation by significant FeCPs formation, disturbances were obviously creating instabilities in co-precipitated and less adsorbed contaminants. However, in 0.1 g systems where remediation is greatly by adsorption into porous FeCPs, disturbances enhanced the formation of FeCPs at high content that were accountable for improved E values.

CHAPTER FIVE

CONCLUSION AND RECOMMENDATIONS

5.1 Conclusion

In metallic iron characterization, the use of only 1,10-Phenanthroline reagent has been proven to be one of the potential Fe^0 characterization methods. When operation and economic aspects are considered, it can be acknowledged to be the most affordable and most straightforward method for the same purpose. The presented Phen method seems to be the most practical and economical method for characterizing the intrinsic reactivity of Fe^0 materials that have as yet been developed. Characterization by EDS, XPS and FESEM of FeCPs before and after fluorine interaction with SW in aqueous systems has proven the existence of reaction that accounts for fluoride removal efficiencies observed in all designed experiments. Furthermore, commendable performances of nano-scale iron-based defluoridation studies provide evidence of metallic iron's potential success in making drinking water free from fluoride contaminations. It has further been associated with many drawbacks, such as interfering co-solutes, undesirable pH values, and other influencing treatments. However, findings from this study show that there is still room for further research over conventional Fe/H_2O systems irrespective of observed inefficiencies from previous similar studies. An approach on quantitative defluoridation using high FeCPs was realized and commented on its unsuitability due to economic feasibility restrictions. Defluoridation by adsorption is preferred as a major means compared to co-precipitation and perhaps size-exclusion; thus, efforts should be emphasized and directed in this approach for prospective pertinent research. Many studies are populated at laboratory batch scale; it is time to transfer this view into column studies and preferably at pilot scale so that observed remarkable findings can prove their validity for public health protection as far as field water decontamination is concerned.

5.2 Recommendations

Future research studies should consider the opportunity and lesson from nano-scale operations, where development of conventional Fe/H_2O filter systems shall exploit the followings:

(i) In-situ coating of sand materials with FeCPs.

(ii) Activation by heat for enhancing the surface area and porosity, a procedure convenient in developing countries as the firing of local ceramic materials are regularly and affordably achieved.

(iii) Realizing short and long term studies for performance breakthroughs and assessing the associated economic feasibility.

REFERENCES

American Public Health Association. (2005). *Standard Methods for the Examination of Water and Wastewater (21st Ed.).* Washington DC: American Public Health Association. https://www.scirp.org/(S(351jmbntvnsjt1aadkozje))/reference/referencespapers.aspx?referenceid=1151995

Apambire, W. B., Boyle, D. R., & Michel, F. A. (1997). Geochemistry, genesis, and health implications of fluoriferous groundwaters in the upper regions of Ghana. *Environmental Geology*, 33(1), 13-24.

Ayoob, S., & Gupta A. K. (2006) Fluoride in Drinking Water: A Review on the Status and Stress Effects. *Critical Reviews in Environmental Science and Technology*, 36(6), 433-487, DOI: 10.1080/10643380600678112

Bårdsen, A., & Bjorvatn, K. (1998). Risk periods in the development of dental fluorosis. *Clinical Oral Investigations*, 2(4), 155-160.

Borgnino, L., Garcia, M. G., Bia, G., Stupar, Y. V., Le Coustumer, P., & Depetris, P. J. (2013). Mechanisms of fluoride release in sediments of Argentina's central region. *Science of the Total Environment,* 443, 245-255.

Brunt, R., Vasak, L., & Griffioen, J. (2004). *Fluoride in groundwater: Probability of occurrence of excessive concentration on global scale, IGRAC*. https://www.google.com

Btatkeu-K, B. D., Tchatchueng, J. B., Noubactep, C., & Caré, S. (2016). Designing metallic iron based water filters: Light from methylene blue discoloration. *Journal of Environmental Management,* 166, 567-573.

Chaturvedi, A. K., Yadava, K. P., Pathak, K. C., & Singh, V. N. (1990). Defluoridation of water by adsorption on fly ash. *Water, Air, & Soil Pollution,* 49(1), 51-61.

Cheremisinoff, P. N., & Morresi, A. C. (1978). *Carbon adsorption applications.* Carbon adsorption handbook. https://www.google.com

Cornell, R. M., & Schwertmann, U. (2003). *The iron oxides: Structure, properties, reactions, occurrences and uses.* John Wiley & Sons. https://www.google.com

Crawford, R. J., Harding, H. L., & Mainwaring, E. D. (1993). Adsorption and coprecipitation of single heavy metal ions onto the hydrated oxides of iron and chromium. *Langmuir*, 9(11), 3050-3056.

Dhillon, A., & Kumar, D. (2019). *New Generation Nano-Based Adsorbents for Water Purification*. https://www.google.com

Duff, M., Coughlin, J., & Hunter, D. (2002). Uranium co-precipitation with iron oxide minerals. *Geochimica et Cosmochimica Acta,* 66(20), 3533-3547.

Fajardo, V., Canto, C., Brown, B., Young, D., & Nesic, S. (2008). *The effect of acetic acid on the integrity of protective iron carbonate layers in CO_2 corrosion of mild steel*. https://www.google.com

Feenstra, L., Vasak, L., & Griffioen, J. (2007). *Fluoride in groundwater: Overview and evaluation of removal methods*. https://scholar.google.com

Ekhard, Z., & Fomon, S. (2000). Fluoride Intake and Prevalence of Dental Fluorosis: Trends in Fluoride Intake with Special Attention to Infants: Review & Commentary. *Journal of Public Health Dentistry,* 60(3), 131-139.

Frencken, J. E. (1992). *Endemic fluorosis in developing countries: Causes, effects and possible solutions.* https://www.google.com

García-Sánchez J. J., Martínez-Miranda V., & Solache-Ríos, M. (2013) Aluminum and calcium effects on the adsorption of fluoride ions by corrosion products. *Journal of Fluorine Chemistry,* 145, 136–140

Gogoi, C., Saikia, J., Sarmah, S., Sinha, D., & Goswamee, R. L. (2018). Removal of fluoride from water by locally available sand modified with a coating of iron oxides. *Water, Air, & Soil Pollution,* 229(4), 118.

Handa, B. K. (1975). Geochemistry and genesis of Fluoride-Containing ground waters in india. *Groundwater,* 13(3), 275-281.

Hari-Kumar, K. V. S., & Singh, Y. (2019). *Skeletal fluorosis*. https://www.google.com

Harrison, J. E., Bayley, T. A., Josse, R. G., Murray, T. M., Sturtridge, W., Williams, C., & Fornasier, V. (1986). The relationship between fluoride effects on bone histology and on bone mass in patients with postmenopausal osteoporosis. *Bone and Mineral*, 1(4), 321-333.

Heimann, S. (2018). *Testing Granular Iron for Fluoride for Aqueous Fluoride Removal*. https://www.google.com

Heimann, S., Ali, Z. P., Lufingo, M., & Ndé-Tchoupé, A. I. (2018a). *Metallic iron for fluoride removal: Starting a research journey*. https://www.google.com

Heimann, S., Ndé-Tchoupé, A. I., Hu, R., Licha, T., & Noubactep, C. (2018b). Investigating the suitability of Fe^0 packed-beds for water defluoridation. *Chemosphere*, 209, 578-587.

Hem, J. D. (1989). *Study and Interpretation of the Chemical Characteristics of Natural Water*. Water Supply Paper 2254, Washington, DC, USA, 3rd edition. https://www.google.com

Henderson, A. D., & Demond, A. H. (2007). Long-term performance of zero-valent iron permeable reactive barriers: A critical review. *Environmental Engineering Science*, 24(4), 401-423.

Hiemstra, T., & Van Riemsdijk, W. H. (2000). Fluoride adsorption on goethite in relation to different types of surface sites. *Journal of Colloid and Interface Science*, 225(1), 94-104.

Huang, Y. H., Shih, Y. J., & Chang, C. C. (2011). Adsorption of fluoride by waste iron oxide: The effects of solution pH, major coexisting anions, and adsorbent calcination temperature. *Journal of Hazardous Materials*, 186(2-3), 1355-1359.

Husain, M., Chavan, F. I., & Bhanudas, A. (2015). Use of Maize husk fly ash as an adsorbent for removal of fluoride. *International Research Journal of Engineering and Technology*, 2(7), 393-401

Hutton, W. L., Linscott, B. W., & Williams, D. B. (1956). Final report of local studies on water fluoridation in Brantford. *Canadian Journal of Public Health*, 47(3), 89-92.

Iiu, Y., Lv, J., Jin, W., & Zhao, Y. (2016). Defluoridation by rice spike-like akaganeite anchored graphene oxide. *Advances*, 6(14), 11240-11249.

Jadhav, A. S., & Jadhav, M. V. (2014). Use of Maize Husk Fly Ash as an Adsorbent for Removal of Fluoride from Water. *International Journal of Recent Development in Engineering and Technology*, 2(2), 41-45.

Jahin, H. S. (2014). Fluoride removal from water using nanoscale zero-valent iron. *International Water Technology Journal*, 4, 173-182

Jolly, S. S., Singh, B. M., Mathur, O. C., & Malhotra, K. C. (1968). Epidemiological, clinical, and biochemical study of endemic dental and skeletal fluorosis in Punjab. *British Medical Journal*, 4(5628), 427-429.

Kimambo, V., Bhattacharya, P., Mtalo, F., Mtamba, J., & Ahmad, A. (2019). *Fluoride occurrence in groundwater systems at global scale and status of defluoridation: State of the art.* Groundwater for Sustainable Development, 100223. hpttps//www.google.com

Kitalika A. J., Machunda R. L., Komakech H. C., & Njau K. N. (2018). Fluoride Variations in Rivers on the Slopes of Mount Meru in Tanzania, *Journal of Chemistry*, 2018, 1-18. doi:10.1155/2018/7140902

Kut, K. M. K., Sarswat, A., Srivastava, A., Pittman, C. U., & Mohan, D. (2016). A Review of Fluoride in African Groundwater and Local Remediation Methods. *Groundwater for Sustainable Development*, 3, 190-212http://dx.doi.org/10.1016/j.gsd.2016.09.001.

Liu, Y., Lv, J., Jin, W., & Zhao, Y. (2016). Defluoridation by rice spike-like akaganeite anchored graphene oxide. *Advances*, 6(14), 11240-11249.

Lottermoser, B. (2003). *Mine wastes Characterization, Treatment and Environmental Impacts. Springer: Berlin. 3rd Ed*. 61, ISBN 978-3-642-12418-1. https//www.google.com

Lufingo, M., Ndé-Tchoupé, A. I., Rui-Hu, R., Njau, K. N., & Noubactep, C. (2019). A novel and facile method to characterize the suitability of metallic iron for water treatment. *Water, 11*(12), 1-14. MDPI AG. Retrieved from http://dx.doi.org/10.3390/w11122465

Makota, S., Nde-Tchoupe, A. I., Mwakabona, H. T., Tepong-Tsindé, R., Noubactep, C., Nassi, A., & Njau, K. N. (2017). Metallic iron for water treatment: Leaving the valley of confusion. *Applied Water Science*, 7, 4177–4196.

Malago, J., Makoba, E., & Muzuka, A. N. N. (2017). Fluoride levels in surface and groundwater in Africa: A review. *American Journal of Water Science and Engineering* 3, 1–17. doi: 10.11648/j.ajwse.20170301.11.

Martínez-Miranda, V., García-Sánchez, J. J., & Solache-Ríos, M. (2011). Fluoride ions behavior in the presence of corrosion products of iron: effects of other anions. *Separation Science and Technology*, 46(9), 1443-1449.

Marwa, J., Lufingo, M., Noubactep, C., & Machunda, R. (2018). Defeating fluorosis in the East African Rift Valley: Transforming the Kilimanjaro into a rainwater harvesting park. *Sustainability*, 10(11), 1-12.

Massé, A., Spérandio, M., & Cabassud, C. (2006). Comparison of sludge characteristics and performance of a submerged membrane bioreactor and an activated sludge process at high solids retention time. *Water Research*, 40(12), 2405-2415.

Mckay, F. S. (1933). Mottled Enamel: The Prevention of Its Further Production through a Change of the Water Supply at Oakley, Ida. *The Journal of the American Dental Association*, 20(7), 1137-1149.

Megha, M., & Meera, V. (2016). Comparison of performance of point of use water treatment systems using various low cost materials for production of drinking water. *International Journal of Innovative Research in Science, Engineering and Technology*, 5, 237–246.

Millar, G. J., Couperthwaite, S. J., Dawes, L. A., Thompson, S., & Spencer, J. (2017). Activated alumina for the removal of fluoride ions from high alkalinity groundwater: New insights from equilibrium and column studies with multicomponent solutions. *Separation and Purification Technology*, 187, 14-24.

Millar, G., Couperthwaite, S., Dawes, L., Thompson, S., & Spencer, J. (2017). Activated alumina for the removal of fluoride ions from high alkalinity groundwater: New insights from equilibrium and column studies with multicomponent solutions. *Separation and Purification Technology*, 187, 14-24.

Btatkeu, K. B. D., Miyajima, K., Noubactep, C., & Caré, S. (2013). Testing the suitability of metallic iron for environmental remediation: Discoloration of methylene blue in column studies. *Chemical Engineering Journal*, 215, 959-968.

Mwakabona, H. T., Ndé-Tchoupé, A. I., Njau, K. N., & Noubactep, C. (2017). Metallic iron for safe drinking water provision: Considering a lost knowledge. *Water Research*, 117, 127-142.

Mwakabona, H. T., Ndé-Tchoupé, A. I., Njau, K. N., Noubactep, C., & Wydra, K. D. (2017). Metallic iron for safe drinking water provision: Considering a lost knowledge. *Water Research*, 117, 127-142.

Nanseu-Njiki, P. C., Noubactep, C., Karoli N. N., & Wydra, K. D. (2017). Making Fe^0-Based Filters a Universal Solution for Safe Drinking Water Provision. *Sustainability*, 9(7), 1-31.

Nath, S. K., & Dutta, R. K. (2015). Significance of calcium containing materials for defluoridation of water: A review. *Desalination and Water Treatment*, 53(8), 2070-2085.

Ndé-Tchoupé, A. I., Crane, R., Mwakabona, H., Noubactep, C., & Njau, K. (2015). Technologies for Decentralized Fluoride Removal: Testing Metallic Iron-based Filters. *Water*, 7(12), 6750-6774.

Ndé-Tchoupé, A. I., Nanseu-Njiki, C. P., Hu, R., Nassi, A., Noubactep, C., & Licha, T. (2019a). Characterizing the reactivity of metallic iron for water defluoridation in batch studies. *Chemosphere*, 219, 855-863.

Ndé-Tchoupé, A. I., Tepong-Tsindé, R., Lufingo, M., Pembe-Ali, Z., Lugodisha, I., Mureth, R. I., & Rahman, M. A. (2019b). White teeth and healthy skeletons for all: The path to universal fluoride-free drinking water in Tanzania. *Water*, 11(1), 1-26.

Ndé-Tchoupé, A., Crane, R., Mwakabona, H., Noubactep, C., & Njau, K. (2015). Technologies for decentralized fluoride removal: Testing metallic iron-based filters. *Water*, 7(12), 6750-6774.

Noubactep, C. (2010). Metallic iron for safe drinking water worldwide. *Chemical Engineering Journal*, 165(2), 740-749.

Noubactep, C. (2011). *Metallic Iron for Safe Drinking Water Production FOG-Freiberg Online Geoscience 27.* https//www.google.com

Noubactep, C. (2013). Metallic iron for water treatment: A critical review. *Clean-Soil, Air, Water,* 41(7), 702-710.

Noubactep, C. (2017). Metallic iron for water treatment: Lost science in the West. *Bioenergetics: Open Access*, 6(01), 1-2.

Noubactep, C. (2018). Metallic iron (Fe^0) provide possible solution to universal safe drinking water provision. *Journal of Water Technology and Treatment Methods*, 1(1), 1-23

Noubactep, C. (2018). Metallic iron for environmental remediation: How experts maintain a comfortable status quo. *Fresenius Environ Bull*, 27, 1379-1393.

Noubactep, C., Schöner, A., & Woafo, P. (2009). Metallic iron filters for universal access to safe drinking water. *Clean-Soil, Air, Water,* 37(12), 930-937.

Noubactep, C., Caré, S., & Crane, R. (2012). Nanoscale metallic iron for environmental remediation: Prospects and limitations. *Water, Air, & Soil Pollution*, 223(3), 1363-1382.

Noubactep, C., Makota, S., & Bandyopadhyay, A. (2017). Rescuing Fe^0 remediation research from its systemic flaws. *Research and Review Insights*, 1(4), 1 – 8. DOI: https:// doi. org/ 10. 15761/RRI

Obiri-Nyarko, F., Grajales-Mesa, S. J., & Malina, G. (2014). An overview of permeable reactive barriers for in situ sustainable groundwater remediation. *Chemosphere*, 111, 243-259.

Parashar, K., Pillay, K., Das, R., & Maity, A. (2019). *Fluoride Toxicity and Recent Advances in Water Defluoridation with Specific Emphasis on Nanotechnology*. https//www.google.com

Pauling L. P. (1960). *The Nature of Chemical Bond and the Structure of Molecules and Crystals: An Introduction to Modern Structural Chemistry*. Cornell University Press, New York, NY, USA. https//www.google.com

People's water. (2017). *The-water-issue-in-Arusha.* https://peopleswater.weebly.com/the-water-issue-in-arusha.html.

Phukan, M. (2015). *Characterizing the ion-selective nature of Fe^0-based systems using azo dyes: Batch and column experiments.* FOG-Freiberg Online Geoscience. https//www.google.com

Ramadan, A., & Hilmi, Y. (2014). *The influence of climate on the determination of the upper permissible fluoride level in potable water in Sudan.* https//www.google.com

Raul, P. K., Devi, R. R., Umlong, I. M., Banerjee, S., Singh, L., & Purkait, M. (2012). Removal of fluoride from water using iron oxide-hydroxide nanoparticles. *Journal of Nanoscience and Nanotechnology,* 12(5), 3922-3930.

Rice, E. W., Baird, R. B., & Eaton, A. D. (2017). *American Water Works Association, American Public Works Association, Water Environment Federation: Standard methods for the examination of water and wastewater.* 23rd Edition. ISBN(s), 9781625762405. Product Code(s), 10086. https//www.google.com

Sakai, K. (2015). *Determination of trace elements in steel using the Agilent 7900 ICP-MS. Agilent publications 5991-6116EN*. https:// www. agilent. com/ cs/ library/ applications/ 5991-6116EN-appnote_7900_ICP-MS_steel_analysis.pdf

Sarkar, M., Banerjee, A., & Pramanick, P. P. (2006). Kinetics and mechanism of fluoride removal using laterite. *Industrial & Engineering Chemistry Research,* 45(17), 5920-5927.

Saxena, V., & Ahmed, S. (2001). Dissolution of fluoride in groundwater: A water-rock interaction study. *Environmental Geology,* (40), 1084-1087.

Silberberg, M. (2012). *Principles of General Chemistry*. McGraw-Hill Education. 2nd Ed, v 1.0. https//www.google.com

Simon, M. J., Beil, F. T., Riedel, C., Lau, G., Tomsia, A., Zimmermann, E. A., & Ignatius, A. (2016). Deterioration of teeth and alveolar bone loss due to chronic environmental high-level fluoride and low calcium exposure. *Clinical Oral Investigations*, 20(9), 2361-2370.

Singh, C., Kumari, R., Singh, R., Shashtri, S., Kamal, V., & Mukherjee, S. (2011). Geochemical modeling of high fluoride concentration in groundwater of Pokhran area of Rajasthan, India. *Bulletin of Environmental Contamination and Toxicology*, 86(2), 152-158.

Sreekanth-Bose, D., Yashoda, R., & Manjunath, P. P. (2018). A review on defluoridation in India. *International Journal of Applied Dental Sciences*, 4(3), 167-171.

Teotia S. P. S., Teotia, M., & Singh, R. K. (1981). Hydro-geochemical aspects of endemic skeletal fluorosis in India: An epidemiologic study. *Fluoride*, 14(2), 69–74.

Tepong-Tsindé, R., Crane, R., Noubactep, C., Nassi, A., & Ruppert, H. (2015). Testing metallic iron filtration systems for decentralized water treatment at pilot scale. *Water*, 7(3), 868-897.

Triszcz, J. M., Porta, A., & Einschlag, F. S. G. (2009). Effect of operating conditions on iron corrosion rates in zero-valent iron systems for arsenic removal. *Chemical Engineering Journal*, 150(2), 431-439.

Velazquez-Jimenez, L. H., Vences-Alvarez, E., Flores-Arciniega, J. L., Flores-Zuniga, H., & Rangel-Mendez, J. R. (2015). Water defluoridation with special emphasis on adsorbents-containing metal oxides and/or hydroxides: A review. *Separation and Purification Technology*, 150, 292-307.

Vodyanitskii, Y. N., & Mineev, V. G. (2015). Degradation of nitrates with the participation of Fe (II) and Fe (0) in groundwater: A review. *Eurasian Soil Science*, 48(2), 139-147.

White, A. F., & Peterson, M. L. (1996). Reduction of aqueous transition metal species on the surfaces of Fe (II)-containing oxides. *Geochimica et Cosmochimica Acta*, 60(20), 3799-3814.

Wong, E. (2017). *Onsite Defluoridation Systems for Drinking Water Production*. https//www.google.com

World Health Organization. (2006). *Fluoride in Drinking-water*. https//www.google.com

World Health Organization. (2011). *Guidelines for Drinking-water Quality*. ISBN: 978 9241548151, WHO Library Cataloguing-in-Publication Data. 4: 370-373. https// www. google. com

Howard, G., Bartram, J., Williams, A., Overbo, A., Geere, J. A., & World Health Organization. (2020). *Domestic water quantity, service level and health*. https//www.google.com

World Health Organization. (2013). *How much water is needed in emergencies. Technical notes on drinking-water, sanitation and hygiene in emergencies*. https//www.google.com

Zhang, C., Li, Y., Wang, T. J., Jiang, Y., & Fok, J. (2017). Synthesis and properties of a high-capacity iron oxide adsorbent for fluoride removal from drinking water. *Applied Surface Science,* 425, 272-281.

Zhu, Q., Li, X., Jiang, Z., & Wei, N. (2015). Impacts of CO_2 leakage into shallow formations on groundwater chemistry. *Fuel Processing Technology*, 135, 162-167.

APPENDICES

Appendix 1: Research output as a publication of a research paper titled: A novel and facile method to characterize the suitability of metallic iron for water treatment

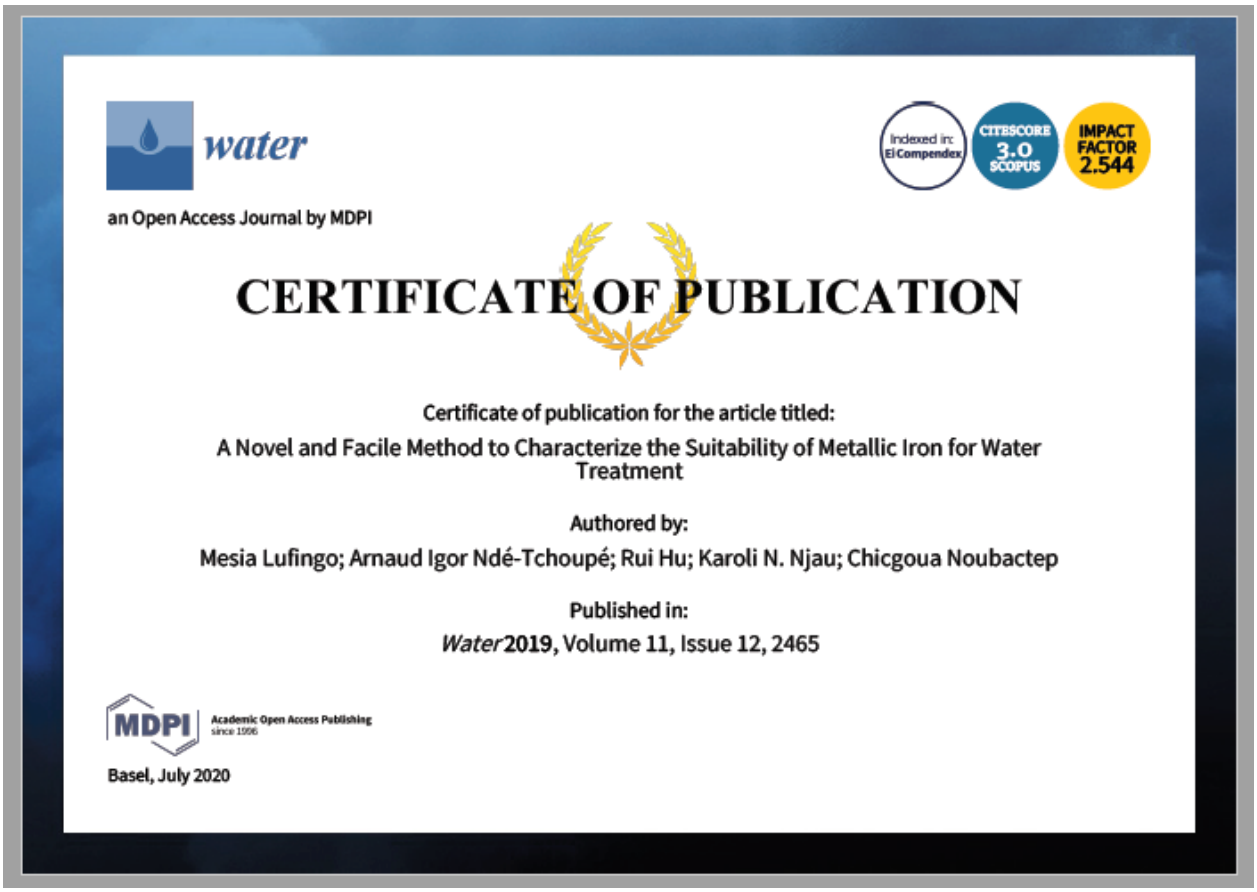

water

an Open Access Journal by MDPI

Indexed in: EI Compendex | CITESCORE 3.0 SCOPUS | IMPACT FACTOR 2.544

CERTIFICATE OF PUBLICATION

Certificate of publication for the article titled:

A Novel and Facile Method to Characterize the Suitability of Metallic Iron for Water Treatment

Authored by:

Mesia Lufingo; Arnaud Igor Ndé-Tchoupé; Rui Hu; Karoli N. Njau; Chicgoua Noubactep

Published in:

Water 2019, Volume 11, Issue 12, 2465

MDPI Academic Open Access Publishing since 1996

Basel, July 2020

Appendix 2: Research output as a publication of a research paper titled: Public water supply and sanitation authorities for strategic sustainable domestic water management. A case of Iringa region in Tanzania

Multidisciplinary Scientific Journal

an Open Access Journal by MDPI

CERTIFICATE OF PUBLICATION

Certificate of publication for the article titled:

Public Water Supply and Sanitation Authorities for Strategic Sustainable Domestic Water Management. A Case of Iringa Region In Tanzania

Authored by:

Mesia Lufingo

Published in:

J **2019**, Volume 2, Issue 4, 449-466

MDPI Academic Open Access Publishing since 1996

Basel, July 2020

Appendix 3: A Summary of average results from Steel Wool Batch Defluoridation in 50 mL Sample Volumes for 2 Days at 23±2 ^{0}C room Temperature

S/N	Systems	Initial	Experimental Condition											
			0.1 g of SW						1.0 g of SW					
			Disturbed			Non-Disturbed			Disturbed			Non-Disturbed		
			pH 4.5	pH 7.0	pH 9.5	pH 4.5	pH 7.0	pH 9.5	pH 4.5	pH 7.0	pH 9.5	pH 4.5	pH 7.0	pH 9.5
1	DW; [F^-]	-	-	-	-	-	-	-	-	-	-	-	-	-
	pH	7.08	6.93	7.6	7.67	6.01	5.95	5.89	6.27	6.28	6.20	5.16	5.48	5.46
	FeCPs (%)	-	-	-	-	-	-	-	-	-	-	-	-	-
2	DW + F; [F^-]	23.9	12.13	14.85	15.30	12.65	14.19	15.62	7.66	7.08	7.51	3.97	4.76	5.7
	% F^- Removal, E	0.00	49.25	37.87	36.00	47.07	40.63	34.64	67.95	70.38	68.58	83.39	80.08	76.15
	pH	7.13	6.32	5.97	6.17	5.95	5.69	5.88	6.46	6.52	6.42	6.03	6.02	5.60
	FeCPs (%)	0	33.6	25.8	24.7	28.5	24.6	21	11.3	11.7	11.6	8.9	8.5	8.1
3	DW + F + Cl; [F^-]	20.40	10.8	15.66	13.95	12.44	13.39	15.3	7.16	7.45	7.73	5.2	4.13	5.69
	% F^- Removal, E	0.00	47.06	23.24	31.62	39.02	34.36	25.00	69.90	63.48	62.11	74.51	79.75	72.11
	pH	6.70	5.99	5.81	5.99	5.80	5.71	5.90	6.38	7.18	6.24	6.25	6.03	6.19
	FeCPs (%)	0	32.1	15.9	21.6	23.6	20.9	15.1	11.6	10.5	10.3	8.0	8.5	7.7
4	DW + F + SO_4; [F^-]	24.80	15.05	15.2	15.95	18.48	17.21	19.91	7.82	9.18	9.18	5.30	7.58	5.21
	% F^- Removal, E	0.00	39.31	38.71	35.69	25.48	30.60	19.72	68.47	62.98	62.98	78.63	69.44	78.99
	pH	6.26	5.84	5.64	5.68	5.85	5.83	5.96	6.43	6.55	6.26	6.11	6.02	5.83
	FeCPs (%)	0	26.8	26.4	24.3	15.3	18.4	11.9	11.4	10.5	10.4	8.4	7.4	8.4
5	DW + F + NO_3; [F^-]	21.90	12.96	16.45	17.65	12.24	15.56	19.15	6.29	7.65	7.06	3.73	2.65	5.30
	% F^- Removal, E	0.00	40.82	24.89	19.41	44.11	28.95	12.56	71.28	65.07	67.76	82.97	87.90	75.80
	pH	5.92	5.58	6.37	6.23	5.84	5.91	6.12	6.34	6.54	6.47	5.98	6.09	6.09
	FeCPs (%)	0	27.8	17	13.2	26.6	17.4	7.6	11.8	10.8	11.2	8.9	9.4	8.1
6	DW + F+HCO_3; [F^-]	23.90	15.25	15.12	16.85	14.83	14.88	18.71	5.40	6.23	7.58	3.54	2.35	3.69
	% F^- Removal, E	0.00	36.19	36.74	29.50	37.95	37.74	21.72	77.41	73.93	68.28	85.19	90.17	84.56
	pH	7.12	6.08	5.92	6.19	6.03	5.82	6.25	6.38	6.27	6.12	5.63	6.17	4.62
	FeCPs (%)	0	24.7	25.1	20.1	22.8	22.7	13.1	12.8	12.3	11.3	9.1	9.6	9.0

7	**DW + F + PO_4; [F^-]**	23.8	16.42	16.37	17.05	18.71	17.83	20.07	6.88	6.33	6.29	3.87	1.44	5.4
	% F^- Removal, E	0.00	31.01	31.22	28.36	21.39	25.08	15.67	71.09	73.40	73.57	83.74	93.95	77.31
	pH	6.90	6.36	6.36	6.54	6.48	6.32	6.59	6.17	6.29	5.72	6.09	5.77	6.26
	FeCPs (%)	0	21.2	21.2	19.3	12.9	15.1	9.4	11.8	12.2	12.2	8.9	10	8.3

RESEARCH OUTPUTS

(i) Journal Publication

Lufingo, M., Ndé-Tchoupé, A. I., Hu, R., Njau, K. N., & Noubactep, C. (2019). A Novel and Facile Method to Characterize the Suitability of Metallic Iron for Water Treatment. *Water*, 11(12), 2465. MDPI AG. Retrieved from http:// dx. doi. org/ 10. 3390/w11122465

(ii) Poster Presentation